

Multimode Resonant Coupling in Pulsating Stars.

Rafał M. Nowakowski

Nicolaus Copernicus Astronomical Center, ul. Bartycka 18, 00-716 Warsaw,
Poland
e-mail: rafaln@camk.edu.pl

ABSTRACT

We consider evolution of an unstable acoustic mode interacting with an ensemble of stable g-modes. We show that the static multimode solution does not exist. We then find the condition for the stability of the statistical equilibrium.

Performing numerical integration of amplitude equations for a simplified system we find that the acoustic mode amplitude exhibits a large irregular variability on the timescale given by the inverse of the growth rate.

The g-mode pairs are excited in significantly wider range of detuning parameters than it is implied by the parametric instability criterion applied to the average amplitude. However, the number of interacting g-mode pairs is reduced because the pairs differing in the detuning parameter by less than their damping rates are synchronized and effectively act as a single pair.

We apply the multimode resonant coupling theory to a realistic stellar model. We choose a seismic model of the δ -Scuti star XX Pyxidis. Although for some $l=2$ modes we find amplitudes of the order of a few millimagnitudes, the typical amplitudes of low-degree modes are much higher. Taking into account the rotational splitting results in decrease of amplitudes by a factor of few which is not enough to obtain consistency with observations. We conclude that in this star and likely in all evolved δ -Scuti stars, the resonant mode coupling cannot be the dominant amplitude limiting effect. The nonresonant saturation of the driving effect must play the role.

Stars: oscillations – Stars: variables: δ Scuti

1 Introduction

In our understanding of stellar multiperiodic variability, which is the typical form of pulsation in main sequence stars and evolved dwarfs, we rely mostly on the linear approximation. This suffices if our aim is calculation of oscillation mode frequencies. Taking into account nonadiabatic effects allows to determine which modes are linearly unstable. This instability usually happens in some ranges of spherical harmonic degrees l and eigenfrequencies. There is fairly good agreement between theoretical frequency ranges of unstable modes and frequencies present in real stars. However, the big unsolved problem is why most of the theoretically unstable modes are not seen in observations. This problem is related to the more general problem of amplitude limitation mechanism, which needs nonlinear approach.

The problem with mode amplitudes concerns in particular δ Scuti stars. Despite the same excitation mechanism as in the giant classical pulsators, namely the κ mechanism, their pulsational behavior is very different and more diverse.

First of all, it was noticed already in seventies (Breger 1979) that only about 30% of stars falling into lower instability strip show detectable variability. This number is somewhat higher today but still less than one half of the stars in the δ Scuti domain are detected as pulsating (Breger 2000a). The large number of variables with amplitudes close to the detection limit suggest that many (perhaps all) of the stars not detected as variable also pulsate but with very small amplitudes.

There is an important subgroup of high-amplitude δ Scuti stars (HADS). Their pulsational properties resemble those of Cepheid-type variables, *i.e.*, only one or two lowest radial modes are present with photometric amplitudes of the order of 0.5 mag. These stars are slowly rotating ($v \sin i \lesssim 30$ km/s) and the oscillation amplitudes are constant or almost constant (see, *e.g.*, Rodriguez 1999). They are more evolved than the rest of the class. However, the majority of δ Scuti stars are low-amplitude pulsators with many independent modes most of which are nonradial. These typical δ Scuti stars can rotate quite fast, with $v \sin i$ up to 250 km/s, but some of them are also slow rotators (Breger 2000a). The pulsation amplitudes of the dominant modes are below 0.1 mag, and those of the remaining modes are usually less than 10 mmag.

Many low-amplitude δ Scuti stars show long-time amplitude modulations. Breger (2000b) analyzed over 30 years of observational data of evolved star 4CVn. The amplitudes of most modes in this star change significantly in the time-scale of ten years or longer. One mode showed rapid decrease of amplitude from 15 mmag in 1974 to 4 mmag in 1976 and 1 mmag in 1977 and later started growing. There was also a phase jump between 1976 and 1977. The amount of amplitude variability in other modes was of the order of 40% during a decade.

A different example is the star XX Pyx that was observed by Handler *et al.* (2000). The observations covered much shorter time, only 125 nights, but due to continuous observation at eight observatories spread around the world and a sophisticated method of nonlinear frequency analysis it was possible to detect amplitude and phase modulations of many modes with the time-scales from 20 to 70 days.

The possible explanation of the apparent difference between pulsational behavior of giant-type pulsators and typical δ Scuti stars involves the resonant mode coupling. The interaction between one higher frequency wave and two lower frequency waves is well known in plasma physics (see, *e.g.*, Davidson 1972). A detailed analysis of general solutions is given by Wersinger *et al.* (1980). In the case of stellar pulsations it was first studied by Vandakurov (1965, 1979). Dziembowski (1982) developed a mathematical formalism suitable to study this kind of interaction in δ Scuti stars. Application of this formalism to a model of ZAMS δ Scuti star (Dziembowski and Królikowska 1985) suggested that the resonant mode coupling indeed was an effective mechanism of amplitude limitation. Dziembowski *et al.* (1988) studied the effects of rotation and showed that the amplitudes could be even smaller than in the nonrotating case. However, all

these studies concerned a stationary situation. In fact, often happens that the stationary solutions are unstable and the dynamical solutions need to be investigated. It was done by Moskalik (1985) in the case of three-mode interaction. The realistic many-mode case was studied only in the context of tidal-capture binaries (Kumar and Goodman, 1996). In that study, the $l=2$ mode had been previously excited due to tidal interaction and the nonlinear couplings caused damping of that mode. It is a different situation than in the case of unstable acoustic modes in δ -Scuti stars, and we cannot strictly apply that study to our case.

2 Parametric Resonance

2.1 The Case of a Single G-Mode Pair

2.1.1 Amplitude Equations

The amplitude equations describing resonant interaction between an acoustic mode with frequency ω_0 and a pair of gravity modes whose frequencies, ω_1, ω_2 , satisfy the condition $|\omega_0 - \omega_1 - \omega_2| \ll \omega_{0,1,2}$ are derived, *e.g.*, by Dziembowski (1982):

$$\frac{dA_0}{d\tau} = \gamma_0 A_0 + i \frac{\epsilon H}{2\sigma_0 I_0} A_1 A_2 e^{-i\Delta\sigma\tau}, \quad (1)$$

$$\frac{dA_{1,2}}{d\tau} = \gamma_{1,2} A_{1,2} + i \frac{H}{2\sigma_{1,2} I_{1,2}} A_0 A_{2,1}^* e^{i\Delta\sigma\tau}, \quad (2)$$

where A are dimensionless complex amplitudes of the interacting modes at the surface, γ denote growth rates, I are moments of inertia, H is the coupling coefficient, and the dimensionless time, τ , and frequencies, σ , are related to the real ones, t, ω by the relation $\tau/t = \omega/\sigma = \sqrt{4\pi G <\rho>}$. The frequency mismatch is given by $\Delta\sigma \equiv \sigma_0 - \sigma_1 - \sigma_2$, and ϵ distinguishes the case of two-mode resonance, where the subscripts 1,2 denote the same mode, and the case of three-mode resonance, where they denote different modes. In the former case $\epsilon=1/2$ and in the latter case $\epsilon=1$. The acoustic mode growth rate is positive and the g-mode growth rates are negative.

Dziembowski (1982) made an explicit use of adiabatic assumption with artificially added growth rates. This yields real coupling coefficient. However, following a derivation procedure of Van Hoolst (1994b), we find the nonadiabatic amplitude equations in very similar form with the complex \mathcal{H}

$$\frac{dA_0}{d\tau} = \gamma_0 A_0 + i \frac{\epsilon \mathcal{H}}{2\sigma_0 I_0} A_1 A_2 e^{-i\Delta\sigma\tau},$$

$$\frac{dA_{1,2}}{d\tau} = \gamma_{1,2} A_{1,2} + i \frac{\mathcal{H}^*}{2\sigma_{1,2} I_{1,2}} A_0 A_{2,1}^* e^{i\Delta\sigma\tau}.$$

If we put $\mathcal{H} = H e^{i\alpha}$ and shift complex phases of g-mode amplitudes by $-i\alpha/2$ the above amplitude equations are reduced to Eqs. (1),(2). Therefore, without

loss of generality, we will use them with real and positive H . Furthermore, we rescale the coupling coefficient

$$C \equiv \frac{H}{\sqrt{\sigma_1 \sigma_2 I_1 I_2}} \quad (3)$$

and the g-mode amplitudes

$$A'_{1,2} \equiv A_{1,2} \sqrt{\frac{\epsilon \sigma_{1,2} I_{1,2}}{\sigma_0 I_0}} \quad (4)$$

in order to obtain simpler form of amplitude equations

$$\frac{dA_0}{d\tau} = \gamma_0 A_0 + i \frac{C}{2} A'_{1,2} A'_{2,1} e^{-i\Delta\sigma\tau}, \quad (5)$$

$$\frac{dA'_{1,2}}{d\tau} = \gamma_{1,2} A'_{1,2} + i \frac{C}{2} A_0 A'_{2,1} e^{i\Delta\sigma\tau}. \quad (6)$$

There are various long timescales which play roles in the evolution of our system. These are the detuning scale, $|\Delta\sigma|^{-1}$, the nonadiabatic scales, $|\gamma|^{-1}$ and the coupling scale $|CA_0|^{-1}$.

If the amplitudes are sufficiently small then only linear terms play role and the amplitude of the acoustic mode grows exponentially. Eventually it reaches the point where the nonlinear terms in Eqs. (6) become important. Assuming sufficiently slow growth of the acoustic mode and using the procedure of Dziembowski (1982) we obtain a criterion for the parametric excitation of the pair of linearly damped g-modes

$$|A_0| > B_{cr} \equiv \sqrt{\frac{4\gamma_1\gamma_2}{C^2} \left[1 + \left(\frac{\Delta\sigma}{\gamma_1 + \gamma_2} \right)^2 \right]}. \quad (7)$$

When the acoustic mode amplitude exceeds the critical value the g-mode amplitudes start to grow and finally the nonlinear term in Eq. (5) can stop the exponential growth of the acoustic mode

In further applications it will be more suitable to use real form of amplitude equations. By substituting

$$A_0 = B_0 e^{i\phi_0}, \quad A'_{1,2} = B_{1,2} e^{i\phi_{1,2}} \quad (8)$$

where B_j are the real and positive amplitudes, and ϕ_j are the real phases of the considered modes, we obtain

$$\frac{dB_0}{d\tau} = \gamma_0 B_0 + \frac{C}{2} B_1 B_2 \sin \Phi, \quad (9)$$

$$\frac{dB_{1,2}}{d\tau} = \gamma_{1,2} B_{1,2} - \frac{C}{2} B_0 B_{2,1} \sin \Phi, \quad (10)$$

$$\frac{d\Phi}{d\tau} = \Delta\sigma + \frac{C}{2} \left[\frac{B_1 B_2}{B_0} - B_0 \left(\frac{B_2}{B_1} + \frac{B_1}{B_2} \right) \right] \cos \Phi, \quad (11)$$

where $\Phi \equiv \Delta\sigma\tau + \phi_0 - \phi_1 - \phi_2$.

2.1.2 Equilibrium Solutions

Here, we repeat the analysis of Dziembowski (1982), who derived the formulae for the equilibrium amplitudes and the criteria for the stability of the equilibrium solution.

If we set l.h.s. of Eqs. (9)–(11) equal to zero we find equilibrium solutions

$$B_0^s = \sqrt{\frac{4\gamma_1\gamma_2}{C^2}(1+q^2)}, \quad (12)$$

$$B_{1,2}^s = \sqrt{\frac{-4\gamma_0\gamma_{2,1}}{C^2}(1+q^2)}, \quad (13)$$

$$\cot \Phi^s = q, \quad (14)$$

where $q = \Delta\sigma/\gamma$, and $\gamma = (\gamma_0 + \gamma_1 + \gamma_2)$.

The stationary solutions describe possible physical state only if they are stable to small perturbations. Linearizing Eqs. (9)–(11) around equilibrium solution (Eqs. 12–14) we have

$$\frac{d}{d\tau} \begin{bmatrix} \delta B_0/B_0 \\ \delta B_1/B_1 \\ \delta B_2/B_2 \\ \delta \Phi \end{bmatrix} = \begin{bmatrix} \gamma_0 & -\gamma_0 & -\gamma_0 & -q\gamma_0 \\ -\gamma_1 & \gamma_1 & -\gamma_1 & -q\gamma_1 \\ -\gamma_2 & -\gamma_2 & \gamma_2 & -q\gamma_2 \\ q(2\gamma_0 - \gamma) & q(2\gamma_1 - \gamma) & q(2\gamma_2 - \gamma) & \gamma \end{bmatrix} \begin{bmatrix} \delta B_0/B_0 \\ \delta B_1/B_1 \\ \delta B_2/B_2 \\ \delta \Phi \end{bmatrix}. \quad (15)$$

The solution of such a linear differential equation is the exponential time dependence $\exp(\lambda\tau)$ and the value of λ is given by the characteristic equation

$$0 = \lambda^4 + a_1\lambda^3 + a_2\lambda^2 + a_3\lambda + a_4, \quad (16)$$

where

$$\begin{aligned} a_1 &= -2\gamma, & a_2 &= \gamma^2(1+q^2) - 4q^2(\gamma_0\gamma_1 + \gamma_0\gamma_2 + \gamma_1\gamma_2), \\ a_3 &= 4\gamma_0\gamma_1\gamma_2(1+3q^2), & a_4 &= -4(1+q^2)\gamma_0\gamma_1\gamma_2\gamma. \end{aligned}$$

The equilibrium solution is stable if the real parts of all eigenvalues λ are negative. This is given by the Hurwitz criteria

$$W_1 = a_1 > 0, \quad W_2 = a_1a_2 - a_3 > 0,$$

$$W_3 = a_3W_2 - a_1^2a_4 > 0, \quad W_4 = a_4W_3 > 0.$$

It can be easily shown that only first and third criteria are independent in our case. They are

$$\gamma = \gamma_0 + \gamma_1 + \gamma_2 < 0, \quad (17)$$

$$4\gamma^3(1+q^2) - (1+3q^2)[4\gamma_0\gamma_1\gamma_2(1+3q^2) + 2\gamma^3(1+q^2) - 8q^2\gamma(\gamma_0\gamma_1 + \gamma_0\gamma_2 + \gamma_1\gamma_2)] > 0. \quad (18)$$

The first criterion says that driving of the p-mode cannot be higher than damping of the g-modes. The second criterion is a quadratic inequality for q^2 . It

is fulfilled if q^2 , and equivalently $|\Delta\sigma|$, is confined to a certain range or if it exceeds certain value.

If $\gamma_0 \ll |\gamma_{1,2}|$, the equilibrium acoustic mode amplitude (Eq. 12) is nearly equal the critical amplitude (Eq. 7). Moreover, according to Wersinger *et al.* (1980), the terminal state is then a stable equilibrium or a periodic limit cycle with average p-mode amplitude close to the equilibrium value. This means that the critical amplitude, given by Eq. (7), may always be treated as an estimate of the acoustic mode amplitude.

2.1.3 Energy Equations

In dynamical considerations it is often useful to use mode energies instead of the amplitudes. The general formula for the energy of an oscillating mode is

$$E = \frac{1}{2} I \sigma^2 |A|^2.$$

The energies in $1/2 I_0 \sigma_0^2$ units in our case are

$$E_0 = |A_0|^2 = B_0^2, \quad (19)$$

$$E_{1,2} = \frac{I_{1,2} \sigma_{1,2}^2}{I_0 \sigma_0^2} |A_{1,2}|^2 \approx \frac{1}{2\epsilon} B_{1,2}^2, \quad (20)$$

where we used Eqs. (4),(8) and we set

$$\sigma_{1,2} \approx \sigma_0/2,$$

because only the modes satisfying this condition play a role.

Now we apply Eqs. (9)–(11) to Eqs. (19),(20) and we obtain

$$\frac{dE_0}{d\tau} = 2\gamma_0 E_0 + 2\epsilon C \sqrt{E_0 E_1 E_2} \sin \Phi, \quad (21)$$

$$\frac{dE_{1,2}}{d\tau} = 2\gamma_{1,2} E_{1,2} - C \sqrt{E_0 E_1 E_2} \sin \Phi, \quad (22)$$

$$\frac{d\Phi}{d\tau} = \Delta\sigma + C \left[\frac{\epsilon \sqrt{E_1 E_2}}{\sqrt{E_0}} - \frac{\sqrt{E_0}}{2} \left(\sqrt{\frac{E_1}{E_2}} + \sqrt{\frac{E_2}{E_1}} \right) \right] \cos \Phi. \quad (23)$$

From these equations we see that the time derivative of the total energy in oscillations is

$$\frac{dE_{total}}{d\tau} = \begin{cases} 2\gamma_0 E_0 + 2\gamma_1 E_1 & \text{for the two-mode resonance} \\ 2\gamma_0 E_0 + 2\gamma_1 E_1 + 2\gamma_2 E_2 & \text{for the three-mode resonance} \end{cases} \quad (24)$$

The coupling terms are only responsible for the energy transfer between the acoustic mode and the gravity modes. Since the growth rates have different signs it is possible to have the solution with constant total energy, *i.e.*, the equilibrium state, or with the total energy varying around some average value, *i.e.*, the limit cycle.

2.1.4 Equal Damping Rates

We noted earlier that the modes in all important g-mode pairs have approximately equal frequencies, $\sigma_1 \approx \sigma_2$. It turns out that their damping rates have the same property, $\gamma_1 \approx \gamma_2 \equiv \gamma_g$. If we assume exact equality we see from Eq. (22) that

$$\frac{d(E_1 - E_2)}{d\tau} = 2\gamma_g(E_1 - E_2).$$

Since $\gamma_g < 0$, the difference between the two energies decays exponentially. Thus, we further assume that the energies, as well as the real amplitudes of the g-modes in each pair are equal. The energy of the pair is

$$E_g = E_1 + E_2 = 2E_1$$

and then we simplify Eqs. (21)–(23)

$$\frac{dE_0}{d\tau} = 2\gamma_0 E_0 + C\sqrt{E_0}E_g \sin \Phi, \quad (25)$$

$$\frac{dE_g}{d\tau} = 2\gamma_g E_g - C\sqrt{E_0}E_g \sin \Phi, \quad (26)$$

$$\frac{d\Phi}{d\tau} = \Delta\sigma + C\left(\frac{E_g}{2\sqrt{E_0}} - \sqrt{E_0}\right) \cos \Phi. \quad (27)$$

Identical equations are obtained in the two-mode resonance case, where $\epsilon = 1/2$ and $E_g = E_1$.

2.2 The Case of Many G-Mode Pairs

The approach adopted by Dziembowski and Królikowska (1985) was to consider an ensemble of g-mode pairs that may be excited through the parametric resonance instability and to determine probability distribution for the p-mode amplitude at onset of the instability. They assumed that the nonlinear interaction with first excited pair will halt the growth of the p-mode amplitude. This could be partially justified when the constant amplitude solution was stable. In the case of the ZAMS star model they considered this was often the case. However, in her unpublished PhD thesis Królikowska showed later that in somewhat evolved objects the interaction with most likely excited g-modes cannot halt the amplitude growth. Therefore, we have to consider the case of many g-mode pairs interacting with the p-mode.

2.2.1 Amplitude Equations

The amplitude equations describing the case of many g-mode pairs are obtained as a straightforward generalization of Eqs. (1),(2)

$$\frac{dA_0}{d\tau} = \gamma_0 A_0 + \sum_{j=1}^N i \frac{\epsilon_j H_j}{2\sigma_0 I_0} A_1^j A_2^j e^{-i\Delta\sigma_j \tau}, \quad (28)$$

$$\frac{dA_{1,2}^j}{d\tau} = \gamma_{1,2}^j A_{1,2}^j + i \frac{H_j}{2\sigma_{1,2}^j I_{1,2}^j} A_0 A_{2,1}^{j*} e^{i\Delta\sigma_j \tau}, \quad (29)$$

where N is the total number of pairs taken into account. Using the same procedure as in the case of a single pair we obtain real amplitude equations

$$\frac{dB_0}{d\tau} = \gamma_0 B_0 + \sum_{j=1}^N \frac{C_j}{2} B_1^j B_2^j \sin \Phi_j, \quad (30)$$

$$\frac{dB_{1,2}^j}{d\tau} = \gamma_{1,2}^j B_{1,2}^j - \frac{C_j}{2} B_0 B_{2,1}^j \sin \Phi_j, \quad (31)$$

$$\frac{d\Phi_j}{d\tau} = \Delta\sigma_j + \sum_{k=1}^N \frac{C_k B_1^k B_2^k}{2B_0} \cos \Phi_k - \frac{C_j}{2} B_0 \left(\frac{B_2^j}{B_1^j} + \frac{B_1^j}{B_2^j} \right) \cos \Phi_j. \quad (32)$$

Now, let us try to find multimode stationary solution of the system. Putting left-hand sides of Eqs. (30)–(32) equal to zero we obtain

$$\gamma_0 B_0 = - \sum_{j=1}^N \frac{C_j}{2} B_1^j B_2^j \sin \Phi_j, \quad (33)$$

$$\gamma_{1,2}^j B_{1,2}^j = \frac{C_j}{2} B_{2,1}^j B_0 \sin \Phi_j, \quad (34)$$

$$\frac{C_j}{2} B_0 \left(\frac{B_2^j}{B_1^j} + \frac{B_1^j}{B_2^j} \right) \cos \Phi_j = \Delta\sigma_j + \frac{1}{B_0} \sum_{k=1}^N \frac{C_k}{2} B_1^k B_2^k \cos \Phi_k. \quad (35)$$

From Eq. (34) we get

$$\frac{C_j}{2} B_0 \frac{B_{2,1}^j}{B_{1,2}^j} = \frac{\gamma_{1,2}^j}{\sin \Phi_j}, \quad (36)$$

and

$$B_1^j B_2^j = \frac{2\gamma_1^j (B_1^j)^2}{B_0 C_j \sin \Phi_j}. \quad (37)$$

From Eqs. (35)–(37) we obtain

$$(\gamma_1^j + \gamma_2^j) \cot \Phi_j = \Delta\sigma_j + \frac{1}{B_0^2} \sum_{k=1}^N \gamma_1^k (B_1^k)^2 \cot \Phi_k. \quad (38)$$

If we multiply Eq. (34) for the mode 1 by the same equation for the mode 2 we get

$$\gamma_1^j \gamma_2^j = \frac{C_j^2}{4} B_0^2 \frac{1}{1 + \cot^2 \Phi_j}. \quad (39)$$

Eqs. (38),(39) form a set of $2N$ equations for $N + 2$ unknowns, namely B_0^2 ,

$$\sum_{k=1}^N \frac{\gamma_1^k (B_1^k)^2 \cot \Phi_k}{C_k},$$

and N values $\cot \Phi_j$. This set has in general no solutions if the number of equations is larger than the number of unknowns. This happens for $N > 2$. We see that the stationary solution exists only if the number of excited pairs is not larger than 2. In further sections we will study time evolution of the mode amplitudes B and phases Φ by means of numerical integration of Eqs. (30)–(32).

2.2.2 Statistical Equilibrium

In the absence of stationary multimode solutions we may still expect that the system will reach some kind of statistical equilibrium. In this section we find a necessary condition for the existence of such a state. We restrict our considerations to the case of equal damping rates in each pair, $\gamma_1^j = \gamma_2^j \equiv \gamma_j$. As we mentioned earlier, this is not far from the relevant realistic situation. Then, similarly as in the case of one g-mode pair, we have $B_1^j = B_2^j \equiv B_j$ and Eqs. (30)–(32) become

$$\frac{dB_0}{d\tau} = \gamma_0 B_0 + \sum_{j=1}^N \frac{C_j}{2} B_j^2 \sin \Phi_j, \quad (40)$$

$$\frac{dB_j}{d\tau} = \gamma_j B_j - \frac{C_j}{2} B_0 B_j \sin \Phi_j, \quad (41)$$

$$\frac{d\Phi_j}{d\tau} = \Delta\sigma_j + \sum_{k=1}^N \frac{C_k B_k^2}{2B_0} \cos \Phi_k - C_j B_0 \cos \Phi_j. \quad (42)$$

Now, we introduce new variables

$$X = B_0^2, \quad Y_j = B_j \sin \Phi_j, \quad Z_j = B_j \cos \Phi_j. \quad (43)$$

Then, from Eqs. (40)–(42) we obtain

$$\dot{X} = 2\gamma_0 X + \sqrt{X} \sum_{k=1}^N C_k Y_k \sqrt{Y_k^2 + Z_k^2}, \quad (44)$$

$$\begin{aligned} \dot{Y}_j &= \gamma_j Y_j - \frac{C_j \sqrt{X}}{\sqrt{Y_j^2 + Z_j^2}} \left(\frac{Y_j^2}{2} + Z_j^2 \right) + \\ &+ Z_j \left(\Delta\sigma_j + \frac{1}{2\sqrt{X}} \sum_{k=1}^N C_k Z_k \sqrt{Y_k^2 + Z_k^2} \right), \end{aligned} \quad (45)$$

$$\dot{Z}_j = \gamma_j Z_j + \frac{C_j \sqrt{X} Y_j Z_j}{2\sqrt{Y_j^2 + Z_j^2}} - Y_j \left(\Delta\sigma_j + \frac{1}{2\sqrt{X}} \sum_{k=1}^N C_k Z_k \sqrt{Y_k^2 + Z_k^2} \right). \quad (46)$$

The divergence of the flow tells us whether the volume in the phase space (X, Y_j, Z_j) evolved by following the orbits obtained from Eqs. (44)–(46) expands or shrinks exponentially. If it expands, the system cannot reach the statistical equilibrium. After some algebra we obtain the divergence of the flow

$$\frac{\partial \dot{X}}{\partial X} + \sum_{j=1}^N \left(\frac{\partial \dot{Y}_j}{\partial Y_j} + \frac{\partial \dot{Z}_j}{\partial Z_j} \right) = 2(\gamma_0 + \sum_{j=1}^N \gamma_j). \quad (47)$$

From this we obtain the necessary condition for the stability of the statistical equilibrium, which is

$$-\sum_{j=1}^N \gamma_j > \gamma_0, \quad (48)$$

i.e., the summed damping rate has to be larger than the acoustic mode driving rate. This is the generalization of the criterion obtained by Wersinger *et al.* (1980) in the case of a single g-mode pair.

In the same way as in the case of a single g-mode pair we derive equations for the time evolution of energies of the interacting modes

$$\frac{dE_0}{d\tau} = 2\gamma_0 E_0 + \sqrt{E_0} \sum_{j=1}^N C_j E_j \sin \Phi_j, \quad (49)$$

$$\frac{dE_j}{d\tau} = 2\gamma_j E_j - \sqrt{E_0} C_j E_j \sin \Phi_j, \quad (50)$$

$$\frac{d\Phi_j}{d\tau} = \Delta\sigma_j + \frac{1}{2\sqrt{E_0}} \sum_{k=1}^N C_k E_k \cos \Phi_k - C_j \sqrt{E_0} \cos \Phi_j, \quad (51)$$

where E_j is the energy of the j -th pair. From Eqs. (49),(50) we see that the time derivative of the total energy in the system is given by

$$\frac{dE_{\text{total}}}{d\tau} = \frac{dE_0}{d\tau} + \sum_{j=1}^N \frac{dE_j}{d\tau} = 2 \left(\gamma_0 E_0 + \sum_{j=1}^N \gamma_j E_j \right). \quad (52)$$

If the damping rates are small compared to the growth rate, the number N of actively interacting g-modes necessary to halt the acoustic mode growth is large, according to Eq. (48). In such a case the system reaches a state with time-dependent and limited amplitudes. The average time derivative of the total energy (Eq. 52) is then equal to zero.

If we assume marginal stability, *i.e.*, the sum of damping rates of all active g-mode pairs is just equal to the acoustic mode growth rate (see. Eq 48), then the total energy derivative (Eq. 52) may be written as

$$\frac{dE_{\text{total}}}{d\tau} = 2 \left(\gamma_0 E_0 + \bar{E}_j \sum_{j=1}^N \gamma_j \right) = 2\gamma_0 (E_0 - \bar{E}_j), \quad (53)$$

where \bar{E}_j is the mean energy of active g-mode pairs, weighted with the damping rates. In the statistical equilibrium the time-averaged total energy derivative is equal zero, which implies

$$\langle E_0 \rangle = \langle \bar{E}_j \rangle. \quad (54)$$

This equation looks like an energy equipartition. In fact, the summed damping is higher than the driving (Eq. 48), so the mean g-mode pair energy is lower than the acoustic mode energy.

One could think that Eq. (54) could be used to estimate the acoustic mode amplitude in the statistical equilibrium. It would be possible if we assumed that active were only pairs which are unstable according to Eq. (7) with the acoustic mode amplitude averaged over the long time. However, it has to be checked numerically whether such an assumption is justified.

3 Time-Dependent Solutions

In this section we analyze time evolution of simple systems. This will help us to understand behavior of modes in realistic stellar model. We will see that there is a qualitative similarity between simple cases and more realistic ones.

3.1 Single G-Mode Pair

The case of a single pair of stable modes was studied in details by Wersinger *et al.* (1980). Here we present two examples of such system.

If the conditions for the stability of the equilibrium solution are satisfied the system reaches this equilibrium. More interesting is the case of unstable equilibrium and stable periodic limit cycle. An example is presented in Fig. 1.

Initially, the amplitudes are low and the acoustic mode amplitude grows according to the linear driving rate. When the amplitude becomes sufficiently high there is significant transfer of energy to the g-mode pair and ultimately the acoustic mode amplitude growth is halted. The evolution proceeds rapidly on the coupling timescale. First, nearly all energy of the p-mode is transferred to the g-mode pair. Then the energy is returned back to the p-mode, but not

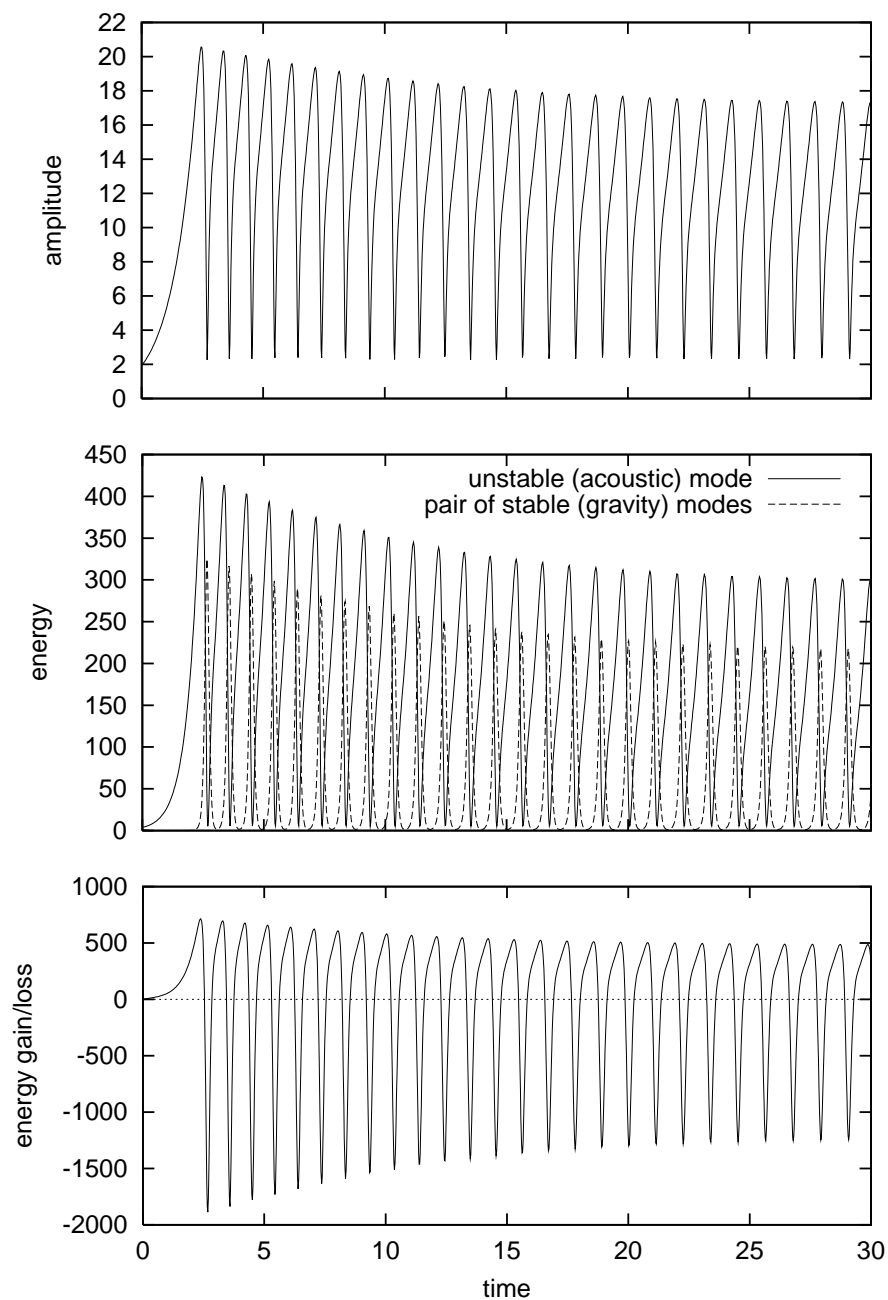


Fig. 1. Time evolution of the system of an unstable (acoustic) mode and a pair of stable (gravity) modes. The parameters are $\gamma_0 = 1$, $\gamma_{1,2} = -3$, $\Delta\sigma = 2$, $C = 1$. Upper panel shows the amplitude of the acoustic mode. Middle panel shows energies of the acoustic mode (solid line) and the g-mode pair (dashed line). Lower panel shows the time derivative of the total energy (Eq. 24). The value of γ_0 sets the unit of time and frequency. The units of amplitudes and energies are set by the value of coupling coefficient.

completely. Part of the energy is dissipated. The state of constant amplitude modulation is reached only after the excess of energy gained in the initial phase is dissipated, *i.e.*, after the time about $20/\gamma_0$. This excess is an artifact of the initial conditions. The mean energy balance (Eq. 52) implies

$$\frac{\langle \bar{E}_g \rangle}{\langle E_0 \rangle} = \frac{\gamma_0}{|\gamma_g|}. \quad (55)$$

The period of the limit cycle is about $1/\gamma_0$. It is so, because the system spends most of the time in the phase of exponential growth of the acoustic mode amplitude. Finally, from the bottom panel we see that the averaged time derivative of the total energy is indeed equal zero.

Fig. 2 presents the case when neither a stable equilibrium nor a stable limit cycle exist. Such a situation takes place, in particular, when condition given by Eq. (48) with $N=1$ is not satisfied. The amplitude growth is unlimited. This growth is modulated in a similar way as in the periodic limit cycle solution, but amplitudes in consecutive cycles are higher and higher. The reason why the situation is unstable is that the g-mode damping is low and the pair does not manage to loose enough energy to balance the unstable mode driving. In lower panel of Fig. 2 it is clearly seen that the average time derivative of the total energy is positive.

We have to add here, that Eq. (48) is not a sufficient condition for the stability. Wersinger *et al.* (1980) showed examples of solutions with unlimited growth despite satisfying this condition for $N=1$ (a single g-mode pair). We found similar cases for $N>1$. What is needed to stop the amplitude growth is some excess of the damping.

3.2 Many G-Mode Pairs

In this section we study the time evolution of a simplified system of interacting modes in the case when several pairs are necessary to halt the acoustic mode growth. We set, as previously, $\gamma_0 = 1$ and $C_j = 1$ for all $N = 19$ pairs. The damping rates are a few times smaller than the growth rate and for all g-modes we set $\gamma_j = -0.3$. The detuning parameters, $\Delta\sigma_j$, are equally spaced between -13.824 and 13.824 with the separation 1.536 . Energies of all interacting modes are shown in Fig. 3 and the time derivative of the total energy is shown in Fig. 4.

At the beginning the acoustic mode amplitude grows exponentially. When the amplitude reaches approximately the critical value given in Eq. (7) the energy transfer begins. The lowest critical amplitude among the pairs in our system is for the one with $\Delta\sigma = 0$ and this pair is excited first. However, this pair alone cannot halt the p-mode growth since the damping rate is too low. Gradually, other pairs are excited, but it takes some time before their amplitudes are large enough to affect the p-mode growth. The initial excess energy is dissipated by modes in a rather wide range of detuning parameters.

Ultimately, after the time of about $15/\gamma_0$ the system achieves the statistical equilibrium in which only 7 closest-to-resonance pairs survive. Let us note that

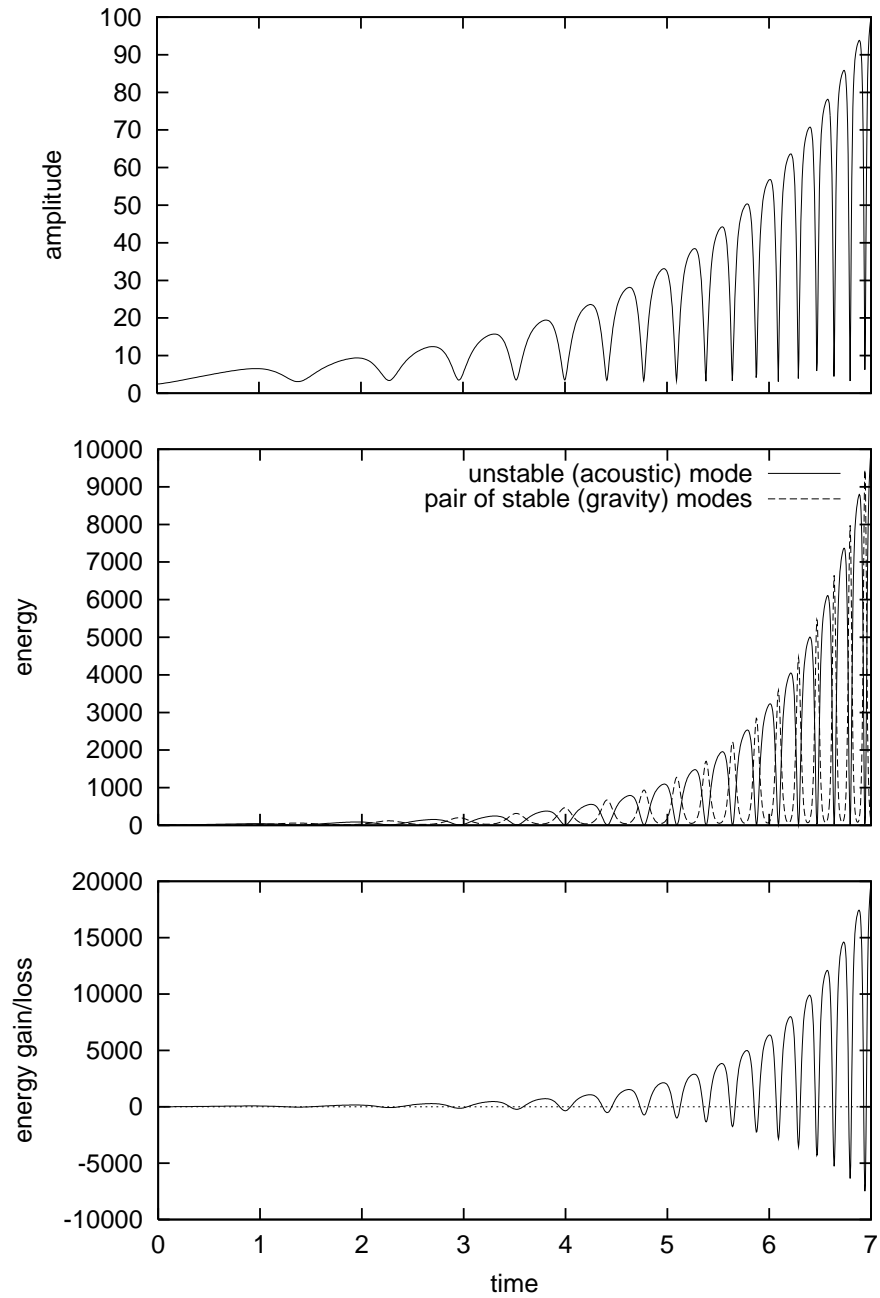


Fig. 2. The same as in Fig. 1 but with parameters that exclude stable solutions, either equilibrium, or limit cycle. The parameters are $\gamma_0 = 1$, $\gamma_{1,2} = -0.4$, $\Delta\sigma = 2$, $C = 1$.

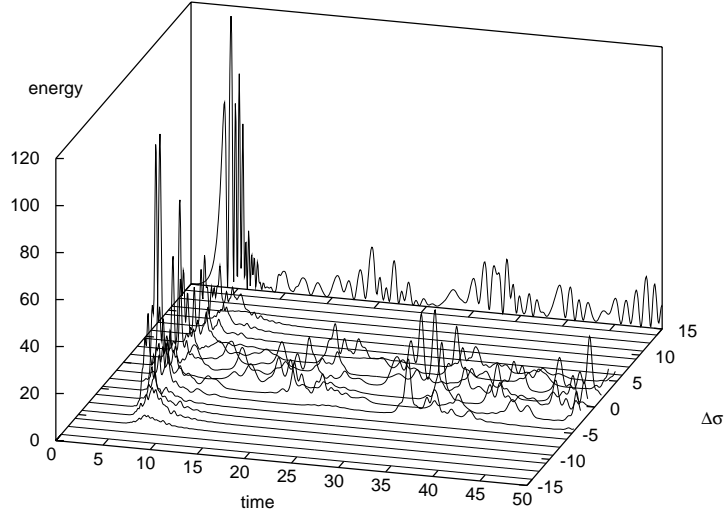


Fig. 3. The time evolution of the multimode system. The energy of the acoustic mode is plotted in the back wall of the 3-D plot. The remaining lines denote energies of g-mode pairs. The detuning parameters of the pairs are equally spaced and the difference between consecutive $\Delta\sigma$'s is 1.536. Other parameters are the same for all pairs, *i.e.*, $\gamma_j = -0.3$, $C_j = 1$. The growth rate of the acoustic mode is $\gamma_0 = 1$. This sets the units of time and frequency. The unit of energy is determined by the value of coupling coefficients. Initial energies of the g-mode pairs are set randomly around the value of 0.01. Initial acoustic mode energy is 0.3.

the number implied by the necessary stability condition (Eq. 48) is 4. The rapid oscillations seen in this phase occur on the timescale determined by the largest detuning parameter of the active pairs and this timescale turns out to be crudely equal to the nonadiabatic timescale γ_0^{-1} . Surprisingly, the result is similar as in the case of a single g-mode pair. This result, which is essential for understanding of amplitude limitation mechanism will be explained in Section 4.

The overall behavior of the acoustic mode is characterized by an irregular variability with a large amplitude modulations. In Fig. 4 we see that the total energy of oscillations is conserved only on average, which means that there is energy exchange with the background.

Fig. 5 presents the energies of active pairs (upper panel) and the energy budget for the acoustic mode (lower panel) in a selected time-interval in the statistical equilibrium phase. What is important, the local energy maxima of various g-mode pairs occur at various times. This lack of synchronization is essential. Synchronized pairs act just as a single pair, as we will show in the next subsection, and they are not efficient energy receivers.

In the lower panel we see that the acoustic mode energy balance is zero on average. The coupling causes an appreciable energy exchange between the

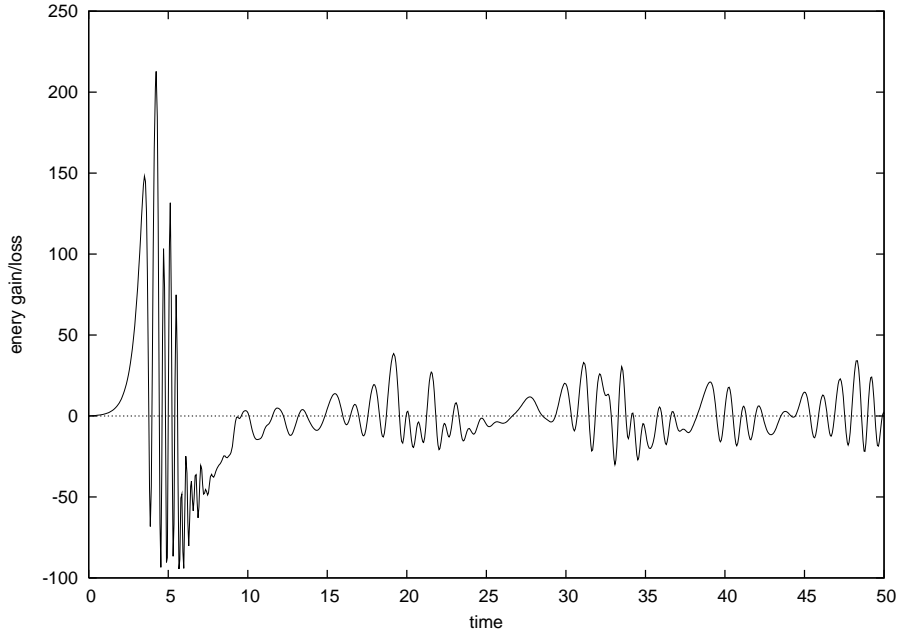


Fig. 4. The time derivative of the total energy in the system shown in Fig. 3.

acoustic and the gravity modes. The net energy transfer necessary to keep the g-modes alive is relatively small.

The rapid and nearly complete energy exchange between the acoustic and the gravity modes, manifested by very large range of amplitude variations, is similar to that in the case of a single g-mode pair. This is so because each individual energy exchange act is typically controlled by a single pair. The irregularity in the present case is caused by involvement of other pairs. In Fig. 5 we see examples when a new pair takes over the control. This happens when the previous pair have low amplitude. Which of the remaining pairs takes the control depends on the relative phase. It must be favorable, *i.e.*, $|A_0| \sin \Phi_j$ must be large negative.

From energy balance (Eq. 52) we obtain

$$\frac{\langle \bar{E}_j \rangle}{\langle E_0 \rangle} = \frac{\gamma_0}{\sum_{j=1}^N |\gamma_j|}, \quad (56)$$

where the summation is done over the active pairs. This is essentially the same result as in the case of a single g-mode pair (see Eq. 55). In our example, the sum of the damping rates of the active pairs is about 2 times higher than the growth rate, γ_0 . Thus, the average g-mode pair energy is about 2 times lower than the average energy of the p-mode.

It is of interest that most of the active g-mode pairs should not be excited according to the parametric instability criterion (Eq. 7) applied to the time-averaged p-mode amplitude. However, the formula for the critical amplitude is

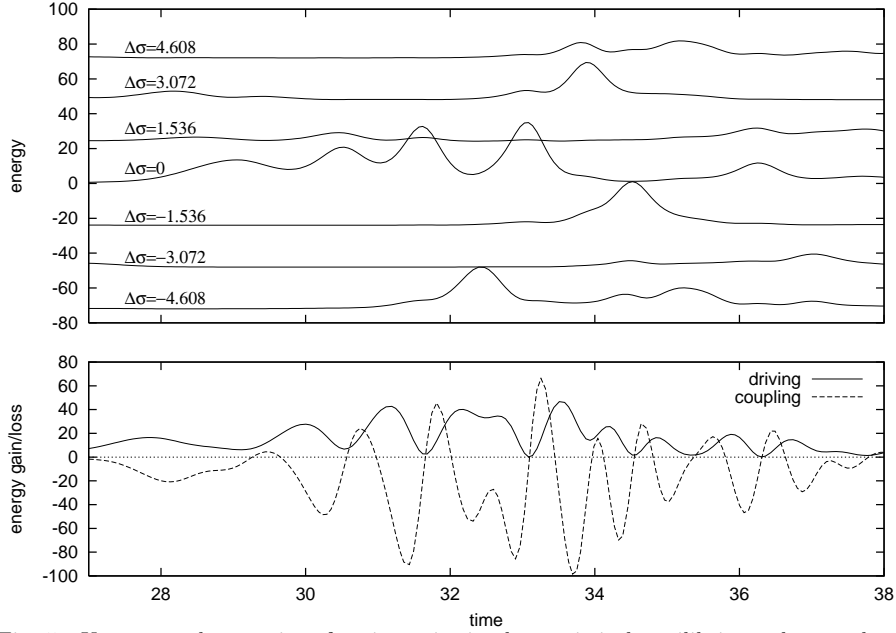


Fig. 5. Upper panel: energies of active pairs in the statistical equilibrium; the zero-levels of the energies are shifted proportionally to $\Delta\sigma$. Lower panel: driving of the acoustic mode (solid line) given by the first term in Eq. (49) and energy transfer to the g-mode pairs due to coupling (dashed line), given by the sum in Eq. (49).

valid only when the p-mode complex amplitude, A_0 , is assumed constant or to vary sufficiently slowly. Here this assumption is not satisfied. One can easily see how the varying A_0 modifies the parametric excitation criterion.

Let us assume $A_0 = A'_0 e^{i\eta\tau}$, and A'_0 is constant. Then, Eq. (2) becomes

$$\frac{dA_{1,2}}{d\tau} = \gamma_{1,2}A_{1,2} + i\frac{H}{2\sigma_{1,2}I_{1,2}}A'_0A_{2,1}^*e^{i(\Delta\sigma+\eta)\tau}, \quad (57)$$

i.e., only detuning parameter is modified. This means the criterion in Eq. (7) becomes

$$|A'_0| = |A_0| > B'_{cr} \equiv \sqrt{\frac{4\gamma_1\gamma_2}{C^2} \left[1 + \left(\frac{\Delta\sigma + \eta}{\gamma_1 + \gamma_2} \right)^2 \right]}. \quad (58)$$

The effective detuning parameter is now $\Delta\sigma + \eta$. In particular, if $\eta = -\Delta\sigma$ the criterion becomes much less restrictive for the pairs with detuning parameter $\Delta\sigma$ than in the case of $A_0 = const$.

In the case presented in Figs. (3)–(5) the amplitude of the acoustic mode varies in a very complicated way. We may treat these variations as consisting of many components oscillating with various frequencies η . A g-mode pair with the detuning parameter $\Delta\sigma_j$ is affected mainly by components with $\eta \approx -\Delta\sigma_j$. This implies that pairs with relatively large detuning parameters may be excited

even when the average acoustic mode amplitude is below the critical value given by Eq. (7). Therefore, we cannot estimate average acoustic mode amplitude in a simple way described at the end of Section 2.

3.3 Pairs with Close Detuning Parameters

When we conducted similar numerical experiments with two or more g-mode pairs having very close detuning parameters, $\Delta\sigma_j$, we observed a synchronization of phases of these pairs. This effect may be demonstrated analytically with the use of Eqs. (40)–(42).

Let us consider two pairs, j_1 , and j_2 with $\Delta\sigma_{j_1} = \Delta\sigma_{j_2}$, as well as $\gamma_{j_1} = \gamma_{j_2} \equiv \gamma$ and $C_{j_1} = C_{j_2} \equiv C$. Then, from Eq. (42), we have

$$\frac{d}{d\tau} \frac{\Phi_{j_1} - \Phi_{j_2}}{2} = CB_0 \frac{\cos \Phi_{j_2} - \cos \Phi_{j_1}}{2} = S \sin \frac{\Phi_{j_1} - \Phi_{j_2}}{2}, \quad (59)$$

where

$$S \equiv CB_0 \sin \frac{\Phi_{j_1} + \Phi_{j_2}}{2}. \quad (60)$$

Upon integration we get

$$\tan \frac{\Phi_{j_1} - \Phi_{j_2}}{4} = \tan \frac{(\Phi_{j_1} - \Phi_{j_2})_0}{4} \exp \left(\int S d\tau' \right). \quad (61)$$

The integrand is a rapidly varying function, but it has a nonzero mean value. This value must be less than zero. To see this let us write Eq. (41) for the two pairs in the form

$$\frac{d \ln B_{j_{1,2}}}{d\tau} = \gamma - \frac{C}{2} B_0 \sin \Phi_{j_{1,2}}. \quad (62)$$

In the statistical equilibrium we have

$$C \langle B_0 \sin \Phi_{j_{1,2}} \rangle = 2\gamma < 0. \quad (63)$$

This holds if both phases $\Phi_{j_{1,2}}$ are in the $(-\pi, 0)$ range when B_0 is large. Then, the average of the two phases, $(\Phi_{j_1} + \Phi_{j_2})/2$, is also in this range during large B_0 phase, implying

$$\langle S \rangle < 0. \quad (64)$$

In fact, the values of the sine functions of both phases as well as of their average, are of the same order, except short periods of time when the phases are close to $0, \pm\pi$. This implies the left-hand side of Eq. (64) to be of the order of 2γ , like in Eq. (63), and the synchronization occurs on the timescale $|\gamma|^{-1}$.

The phase synchronization has an important consequence for the multimode coupling. We may replace in Eqs. (49)–(51) the energies of the pairs with the same Φ , γ , C , and $\Delta\sigma$ by the sum of their energies. Then, the equations for the other pairs remain unchanged. This means that the synchronized pairs act effectively as a single pair and in this way we may reduce the number of pairs and the number of equations to solve.

In a more realistic situation, the two pairs do not have exactly equal detuning parameters. Then, instead of Eq. (59) we have

$$\frac{d}{d\tau} \frac{\Phi_{j_1} - \Phi_{j_2}}{2} = \frac{\Delta\sigma_{j_1} - \Delta\sigma_{j_2}}{2} + S \sin \frac{\Phi_{j_1} - \Phi_{j_2}}{2}. \quad (65)$$

When we use Eq. (64), then Eq. (65) becomes

$$\frac{d}{d\tau} \frac{\Phi_{j_1} - \Phi_{j_2}}{2} \approx \frac{\Delta\sigma_{j_1} - \Delta\sigma_{j_2}}{2} + 2\gamma \sin \frac{\Phi_{j_1} - \Phi_{j_2}}{2}. \quad (66)$$

It's solution is

$$\tan \frac{\Phi_{j_1} - \Phi_{j_2}}{4} = \frac{1}{z} - \frac{1}{z} \sqrt{1 - z^2} \tanh \left(\sqrt{1 - z^2} |\gamma| (\tau + T) \right), \quad (67)$$

where $z = (\Delta\sigma_{j_1} - \Delta\sigma_{j_2}) / (4|\gamma|)$, and T is the integration constant whose value is determined by the initial conditions. If $|z| \ll 1$ then for $\tau \rightarrow \infty$ we get

$$\Phi_{j_1} - \Phi_{j_2} \approx 2z = \frac{\Delta\sigma_{j_1} - \Delta\sigma_{j_2}}{2|\gamma|}. \quad (68)$$

We see now, that the phases are synchronized if the difference of detuning parameters is much less than $|\gamma|$. In fact, we found in numerical experiments that the pairs may be treated as synchronized if the $\Delta\sigma$ difference is just smaller than γ . Only for larger difference the pairs are really independent.

The synchronization has important consequence for the stability condition (Eq. 48) in which we should count only independent pairs.

4 General Properties of Multimode Solutions

In the previous section we studied systems where all pairs had the same damping rates and coupling coefficients. It turns out, however, that the main qualitative properties of the multimode solutions are valid also in more realistic systems, where the pairs have various damping rates and coupling coefficients.

Firstly, the pairs are excited in significantly wider range of $\Delta\sigma$ than implied by Eq. (7) with the acoustic mode amplitude replaced by its average value. Secondly, the pairs with very close detuning parameters are synchronized. Thirdly, the p-mode amplitude is very strongly modulated due to nearly complete energy transfer between the interacting modes. Finally, the modulation timescale is given by the inverse of the growth rate γ_0 .

The wide range of detuning parameters of active pairs is the result of rapidly varying amplitude of the acoustic mode (see Subsection 3.2.2).

The pairs with close detuning parameters and equal damping rates and coupling coefficients are synchronized, as was shown in Subsection 3.3. It turns out that the pairs with different damping rates and/or coupling coefficients also tend to synchronization if their detuning parameters differ less than the smaller

of their damping rates. In such a case, in a statistical equilibrium, we have

$$\langle B_0 \sin \Phi_{j_1} \rangle = \frac{2\gamma_{j_1}}{C_{j_1}}, \quad (69)$$

$$\langle B_0 \sin \Phi_{j_2} \rangle = \frac{2\gamma_{j_2}}{C_{j_2}}, \quad (70)$$

(see Eq. 63). The synchronization causes both left-hand sides of above equations to be roughly equal. If the right-hand sides differ significantly, it is obvious that these equations cannot be satisfied simultaneously. Only the one with lower value of $|\gamma/C|$ can be satisfied, because the sine functions have limited values. The energy transfer to the g-mode pair with higher $|\gamma/C|$ is inefficient and this pair gets damped. This means that we may treat such pairs as one effective pair, like in the case of equal damping rates and coupling coefficients. Here, this effective pair is just the one with the smallest $|\gamma/C|$ ratio.

The large amplitude modulation is the result of nearly complete energy exchange between the p-mode and the g-mode pair that currently controls the interaction. The mode energies averaged over all active pairs and over a long time satisfy Eq. (56). However, if we have groups of synchronized pairs, each group has to be counted as a single pair. We expect, just as in the simplified case considered in the previous section, that the average energy of the g-modes is a few times lower than the average p-mode energy.

The fact that the amplitude modulation timescale is of the order of γ_0^{-1} is caused by the synchronization of the g-mode pairs with close detuning parameters and the stability criterion given by Eq. (48). In a realistic situation the damping rates of the active g-mode pairs are much smaller than the driving rate of the acoustic mode. This means that the number of active pairs is high, namely it has to be higher than $N_{min} = \gamma_0/|\bar{\gamma}_j|$ (see Eq. 48), where $\bar{\gamma}_j$ is the mean value of the damping rate of the active pairs. Moreover, the independent active pairs have to be separated in the $\Delta\sigma$ space by more than $|\bar{\gamma}_j|$. This implies the range of detuning parameters occupied by active pairs have to be larger than $N_{min}|\bar{\gamma}_j| = \gamma_0$. The maximum $\Delta\sigma$ of the active pairs, which gives the shortest modulation timescale, is thus higher than $\gamma_0/2$. In fact, it should be typically equal to a few times γ_0 .

5 Application to a Realistic Stellar Model

5.1 The Model

Numerical study of oscillation in a realistic situation must begin with model construction. In our work we adopted one of possible models of the δ Scuti star XX Pyxidis calculated by Pamyatnykh *et al.* (1998). Our choice is motivated, in part, by the interesting data that we have for this object and, in part, by the fact that the star is a moderately evolved object, just like most of the well studied δ Scuti stars.

The model mass is $1.9M_{\odot}$, radius $2.06R_{\odot}$, effective temperature $8045K$, and luminosity $15.8L_{\odot}$. The model is slightly evolved, the central hydrogen abundance is 0.39. No rotation is assumed.

We computed nonadiabatic acoustic modes in our model. The unstable modes of $l \leq 2$ are found in the frequency range $3.7 \lesssim \sigma \lesssim 6.2$. The most important parameters of the modes are listed in Table 1. Additionally, the growth rates

Table 1
Parameters of unstable acoustic modes

l	σ	$P[\text{min}]$	γ
0	3.909	52.91	1.455e-05
0	4.544	45.52	1.096e-04
0	5.201	39.77	3.527e-04
0	5.859	35.30	4.869e-04
1	4.125	50.15	3.758e-05
1	4.815	42.96	2.005e-04
1	5.495	37.64	4.812e-04
1	6.162	33.57	2.194e-04
2	3.725	55.53	3.041e-06
2	3.883	53.27	4.134e-06
2	4.440	46.59	8.830e-05
2	5.120	40.40	3.243e-04
2	5.793	35.71	5.106e-04

of the acoustic modes versus their frequencies are shown in Fig. 6. We will also use another linear characteristics of the modes, the complex factor f , which is the ratio of relative flux to relative radius variations. The absolute values of this factor are close to 30 for all the modes listed in Table 1.

5.2 Gravity Modes

The properties of g-modes are determined by the behavior of the Brunt-Väisälä frequency. It is presented in Fig. 7. Here we summarize the more general discussion presented by Dziembowski (1982) and Dziembowski and Królikowska (1985).

Gravity modes can propagate in a region where their frequencies are lower than the Brunt-Väisälä frequency (g-mode propagation zone) and this region have to be surrounded by evanescent zones where the Brunt-Väisälä frequency is lower. The frequencies of the g-modes that are efficiently coupled to the acoustic mode are close to one half of its frequency. Thus, as we may see in Table 1, the interesting gravity modes have frequencies between about 1.8 and 3.1. We see in Fig. 7 that there are two separate propagation zones for such frequencies, one extending from $r/R \approx 0.1$ to $r/R \approx 0.4 \div 0.5$, and another in the range $0.95 \lesssim r/R \lesssim 0.98^*$. Therefore, we have to consider two sets of g-modes of

*In fact there is another, very narrow, propagation zone at $r/R < 0.1$ for modes with $\sigma \gtrsim 3$,

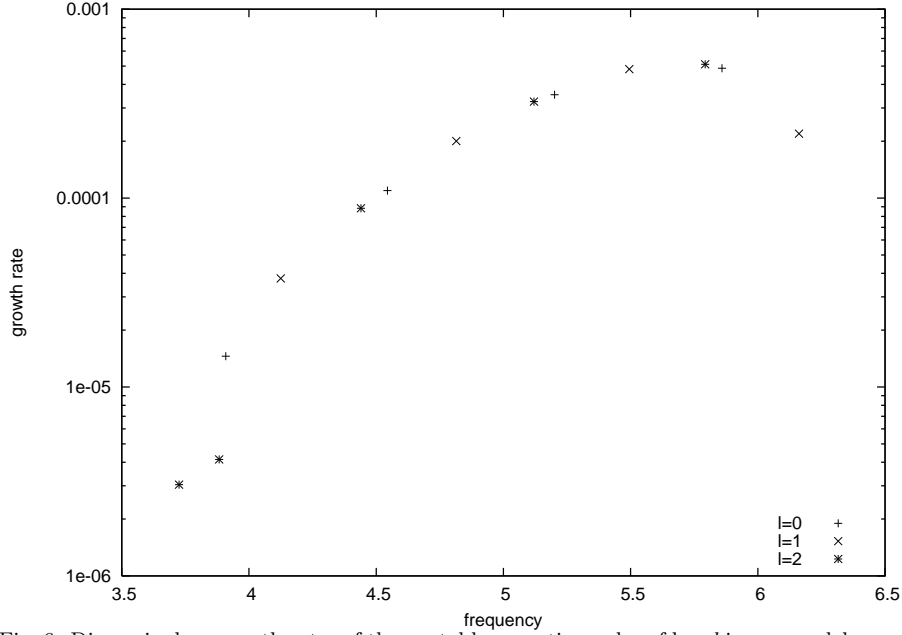


Fig. 6. Dimensionless growth rates of the unstable acoustic modes of low- l in our model versus their dimensionless frequencies.

vastly different properties.

The inner g-modes can be studied in the asymptotic approximation (see, *e.g.*, Dziembowski 1982, Van Hoolst *et al.* 1998). It is valid when the wavelength of the mode is much shorter than the local hightscale. The radial wavenumber of a mode k is given by

$$k_k = \frac{\kappa_k}{r} = \frac{1}{r} \sqrt{\Lambda_k \left(\frac{\mathcal{N}_{BV}^2}{\sigma_k^2} - 1 \right)}, \quad (71)$$

where \mathcal{N}_{BV} is the dimensionless Brunt-Väisälä frequency, and $\Lambda_k = l_k(l_k + 1)$. The displacement, $\boldsymbol{\eta}_k$, is expressed in the form

$$\boldsymbol{\eta}_k(\mathbf{r}, \tau) = \boldsymbol{\xi}_k(\mathbf{r}) A_k e^{i\sigma_k \tau}, \quad (72)$$

where the eigenvector

$$\boldsymbol{\xi}_k(\mathbf{r}) = (y_{1,k}(r) \mathbf{e}_r + z_k(r) \nabla_H) Y_{l_k}^{m_k}(\theta, \phi). \quad (73)$$

The radial eigenfunctions in the asymptotic approximation are given by

$$y_{1,k}(r) = \frac{f_k(r)}{r^3 \sqrt{\rho}}, \quad (74)$$

$$z_k(r) = \frac{1}{\Lambda_k r^3 \sqrt{\rho}} \left(\frac{df_k(r)}{d \ln r} + f_k(r) \frac{\mathcal{A} - V_g}{2} \right), \quad (75)$$

but this has no practical meaning.

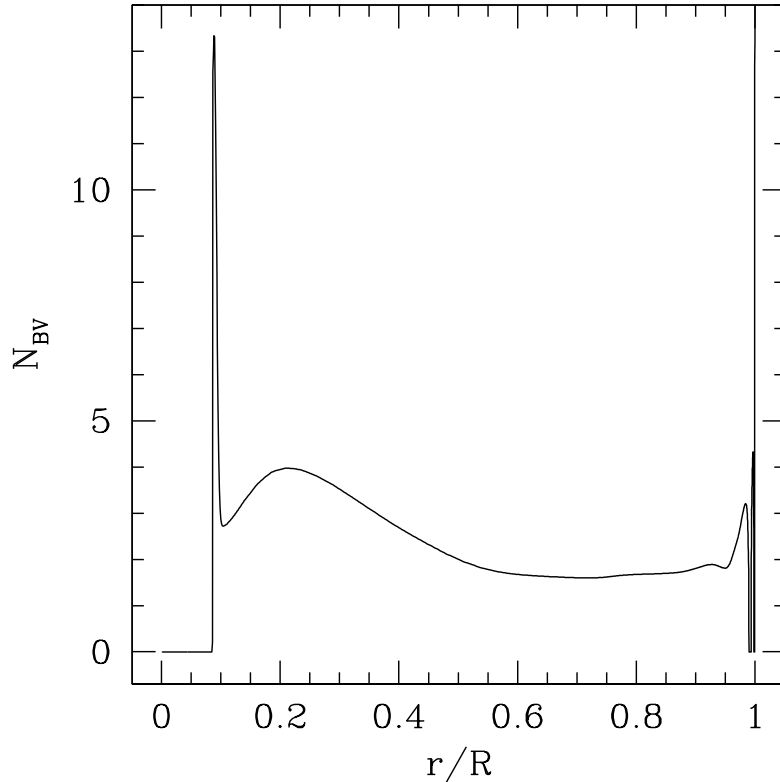


Fig. 7. The dimensionless Brunt-Väisälä frequency versus radius in the adopted model. The atmospheric values are about 30.

where

$$f_k(r) = \mathcal{D}_k \sqrt{r/\kappa_k} \sin \psi_k, \quad \psi_k = \int \kappa_k d \ln r, \quad (76)$$

the structure functions \mathcal{A} and V_g are given by

$$V_g = \frac{V}{\Gamma} = -\frac{1}{\Gamma} \frac{d \ln p}{d \ln r}, \quad \mathcal{A} = -\frac{d \ln \rho}{d \ln r} - V_g, \quad (77)$$

Γ is the adiabatic exponent and remaining symbols have traditional meaning. When the mode degree l_k is high so is the radial wavenumber, implying high radial order, n_k . In such a case a small change of the frequency is sufficient to change the order n by one, which means the spectral density of g-modes is very high. Thus, for each l it is quite easy to find a pair satisfying the resonant condition. We find in our model that the frequency distance between inner g-modes of a given l and consecutive n 's, for the modes that are interesting for us, can be approximated by

$$\delta \sigma_{l,n} \equiv \sigma_{l,n} - \sigma_{l,n+1} \approx \frac{0.36 \sigma_{l,n}}{l}. \quad (78)$$

The inner g-modes are quasiadiabatic which means the only important non-adiabatic quantity is the damping rate. In this approach it may be approximated by

$$-\gamma_k = \frac{\Lambda_k}{\sigma_k^2 \tau_{th}}, \quad (79)$$

where τ_{th} is the thermal timescale of the inner g-mode cavity. In our case it is roughly equal to 10^{10} , which implies the damping rates of the relevant modes range from 3×10^{-8} at $l \sim 40$ to 2×10^{-5} at $l \sim 1000$. Thus, the stability criterion given by Eq. (17) is not satisfied, because the driving rates of the acoustic modes, given in Table 1, are typically much higher. It is necessary to take into account at least several g-mode pairs to satisfy Eq. (48). As was shown in Subsection 2.2.1, this implies that the coupling to the inner g-modes cannot result in constant amplitude p-mode pulsation.

Neither asymptotic nor quasiadiabatic approximation can be applied to modes trapped in the outer g-mode cavity. These outer g-modes still have relatively high degrees l but, because of the narrowness of the cavity, the radial orders n are low, typically 1 or 2. The nonadiabatic damping rates of these modes are typically between about 0.02 at $\sigma_{1,2} \lesssim 2.1$ and about 0.5 at $\sigma_{1,2} \gtrsim 2.8$. The strong damping of these modes might suggest they are not likely to be excited. However, the coupling coefficients are also orders of magnitude larger than in the case of the inner g-modes, and the critical amplitudes given by Eq. (7) can be comparable to those for the latter. Neither in this case we expect a stationary pulsation because the second of the stability criteria (Eq. 18) is not fulfilled because he have $q^2 \ll 1$ and $\gamma_0 \ll |\gamma_{1,2}|$. Since the criteria given by Eq. (17) as well as Eq. (48) with $N = 1$ are satisfied and the damping rates are much higher than the growth rates, a single outer g-mode pair is sufficient to halt the acoustic mode growth. The instability of the stationary solution in this case implies that the system reaches a limit cycle solution.

In cooler δ Scuti stars p-mode driving extends to lower frequencies, such that the resonant g-modes have their frequencies below the \mathcal{N}_{BV} minimum. In this case the g-modes propagate through the whole radiative interior. Clearly the spectrum of such modes is very dense and damping is intermediate between that of the inner and the outer g-modes.

5.3 The Coupling Coefficient

Various authors give various expressions for the coupling coefficient. While the form of equations is basically always the same, the coupling coefficient may be expressed in various equivalent ways whose equivalence is not always apparent. Moreover, different formulae have different numerical properties and it is not an easy task to choose the best one. We restrict ourselves here to adiabatic formulae for two reasons. Firstly, there is no nonadiabatic formulae in literature available to us. Secondly, in the inner cavity the modes are indeed nearly adiabatic, yielding the adiabatic coupling coefficient to be an excellent approximation. This is not true for the outer g-modes. Therefore, we should treat the results

obtained for them as rough estimates. We will also discuss the effects of possible negligible coupling to these modes.

The most detailed derivation of the adiabatic nonlinear oscillation equations and the formula for the coupling coefficient is given by Van Hoolst (1993, 1994a). This formula clearly shows symmetry properties of the coefficient, but it is not good for numerical calculations in the case of high-order modes because there are many big terms canceling each other. Numerically much better formula of Dziembowski (1982) has a problem with treating the sharp peak of the Brunt-Väisälä frequency slightly below $r = 0.1R$ (see Fig. 7). The most appropriate for us seems to be the formula derived by Kumar and Goodman (1996). Transformed to our notation it takes the following form

$$H = \frac{1}{8\pi G \langle \rho \rangle} \int \mathcal{L}_3 dV, \quad (80)$$

where H is the coupling coefficient introduced in Eqs. (1),(2). The integration is done over the stellar volume, and the third-order Lagrangian is given by

$$\begin{aligned} \mathcal{L}_3 = & \xi_{0;i}^j \xi_g^i p'_{g;j} - \frac{1}{2} (p'_{0;i;j} + \rho \Psi'_{0;i;j}) \xi_g^i \xi_g^j - p'_{0;i} \xi_g^i \operatorname{div} \xi_g - \frac{1}{2} p'_0 (\operatorname{div} \xi_g)^2 + \\ & + \frac{\Gamma(\Gamma-2)}{2} p \operatorname{div} \xi_0 (\operatorname{div} \xi_g)^2 - \frac{1}{2} p_{;i} \xi_0^i (\operatorname{div} \xi_g)^2 - p_{;i} \xi_g^i \operatorname{div} \xi_g \operatorname{div} \xi_0 - \\ & - p_{;i;j} \left(\frac{1}{2} \xi_g^i \xi_g^j \operatorname{div} \xi_0 + \xi_g^i \operatorname{div} \xi_g \xi_0^j \right) - \frac{1}{2} (p_{;i;j;k} + \rho \Psi_{;i;j;k}) \xi_0^i \xi_g^j \xi_g^k. \quad (81) \end{aligned}$$

In the last expression ξ_0 is the acoustic mode eigenvector and the ξ_g symbol denotes the sum of the gravity mode eigenvectors. The semicolons denote the covariant derivatives, upper indices denote contravariant vector components,

$$p'_a = -\xi_a \cdot \nabla p - \Gamma p \operatorname{div} \xi_a$$

is the Eulerian pressure perturbation of the mode a , Ψ is the gravitational potential, and Ψ'_0 is its Eulerian perturbation of the acoustic mode. We make use of the Cowling approximation for the g-modes, $\Psi'_1 = \Psi'_2 = 0$.

We introduce eigenfunction

$$y_{2,k} = z_k \mathcal{C} \sigma_k^2,$$

where $\mathcal{C} = 3(r/R)^3 M/M_r$ and M_r is the mass in a sphere of the radius r^\dagger . Additionally, for the acoustic mode we introduce eigenfunctions $y_{3,0}, y_{4,0}$ defined by

$$\begin{aligned} \Psi'_0 &= gr y_{3,0} Y_0 \\ \frac{d\Psi'_0}{dr} &= gy_{4,0} Y_0. \end{aligned}$$

[†]Note that \mathcal{A}/\mathcal{C} is the square of the dimensionless Brunt-Väisälä frequency \mathcal{N}_{BV} .

Then we substitute eigenfunctions into Eq. (81), keep only terms with products of the functions of three different modes (only such terms contribute to the resonant coupling), and after very long and tedious algebra we obtain finally

$$\begin{aligned}
H = & \frac{Z}{2} \int \frac{\rho r^4 dr}{\mathcal{C}} \left\{ y_{1,1} y_{1,2} \left[y_{1,0} \left(\mathcal{A} (4 + \mathcal{C} \sigma_0^2 - U - V_g) + 2\mathcal{C} \sigma_1 \sigma_2 (2 - V_g) \right) + \right. \right. \\
& \left. \left. + y_{2,0} (\mathcal{A} + 2\mathcal{C} \sigma_1 \sigma_2) \left(V_g - \frac{\Lambda_0}{\mathcal{C} \sigma_0^2} \right) - y_{3,0} V_g (\mathcal{A} + 2\mathcal{C} \sigma_1 \sigma_2) - y_{4,0} \mathcal{A} \right] + \right. \\
& + y_{1,1} y_{2,2} \left[y_{1,0} \left(V_g (4 + \mathcal{C} \sigma_0^2 - U - V) - \frac{\Lambda_0 + \Lambda_2 - \Lambda_1}{2} \left(\frac{\mathcal{A}}{\mathcal{C} \sigma_0^2} + 2 \frac{\sigma_1}{\sigma_2} \right) \right) + \right. \\
& \left. + y_{2,0} \left(V_g \left(V - \frac{\Lambda_0}{\mathcal{C} \sigma_0^2} \right) + \frac{\Lambda_0 + \Lambda_2 - \Lambda_1}{2} \left(\frac{\mathcal{A} - 1}{\mathcal{C} \sigma_0^2} + \frac{1 - \mathcal{C} \sigma_1^2}{\mathcal{C} \sigma_2^2} \right) \right) - \right. \\
& \left. - y_{3,0} V V_g - y_{4,0} V_g \right] + \\
& + y_{2,1} y_{1,2} \left[y_{1,0} \left(V_g (4 + \mathcal{C} \sigma_0^2 - U - V) - \frac{\Lambda_0 + \Lambda_1 - \Lambda_2}{2} \left(\frac{\mathcal{A}}{\mathcal{C} \sigma_0^2} + 2 \frac{\sigma_2}{\sigma_1} \right) \right) + \right. \\
& \left. + y_{2,0} \left(V_g \left(V - \frac{\Lambda_0}{\mathcal{C} \sigma_0^2} \right) + \frac{\Lambda_0 + \Lambda_1 - \Lambda_2}{2} \left(\frac{\mathcal{A} - 1}{\mathcal{C} \sigma_0^2} + \frac{1 - \mathcal{C} \sigma_2^2}{\mathcal{C} \sigma_1^2} \right) \right) - \right. \\
& \left. - y_{3,0} V V_g - y_{4,0} V_g \right] + \\
& + y_{2,1} y_{2,2} \left[y_{1,0} \left(V_g^2 (\Gamma - 1) - V_g \left(\frac{\Lambda_0 + \Lambda_1 - \Lambda_2}{2\mathcal{C} \sigma_1^2} + \frac{\Lambda_0 + \Lambda_2 - \Lambda_1}{2\mathcal{C} \sigma_2^2} \right) - \right. \right. \\
& \left. \left. - \frac{\Lambda_1 + \Lambda_2 - \Lambda_0}{\mathcal{C} \sigma_1 \sigma_2} \right) + \right. \\
& \left. + y_{2,0} \left(V_g^2 (1 - \Gamma) + V_g \left(\frac{\Lambda_0 + \Lambda_1 - \Lambda_2}{2\mathcal{C} \sigma_1^2} + \frac{\Lambda_0 + \Lambda_2 - \Lambda_1}{2\mathcal{C} \sigma_2^2} \right) + \right. \right. \\
& \left. \left. + \frac{(\Lambda_1 - \Lambda_2)^2 - \Lambda_0^2}{2\mathcal{C}^2 \sigma_0^2 \sigma_1 \sigma_2} \right) + \right. \\
& \left. + y_{3,0} \left(V_g^2 (\Gamma - 1) - V_g \left(\frac{\Lambda_0 + \Lambda_1 - \Lambda_2}{2\mathcal{C} \sigma_1^2} + \frac{\Lambda_0 + \Lambda_2 - \Lambda_1}{2\mathcal{C} \sigma_2^2} \right) \right) \right] \left. \right\}, \quad (82)
\end{aligned}$$

where

$$Z = \int Y_0^* Y_1 Y_2 d\Omega, \quad U = \frac{4\pi \rho r^3}{M_r}.$$

If the acoustic mode is radial the linear Eulerian perturbation of the gravitational potential can be obtained analytically and the function $y_{2,0}$ has a different meaning than for the nonradial modes. It changes a bit the final formula for the coupling coefficient. It turns out, however, that if we put $y_{3,0} = 0$ and $y_{4,0} = -U y_{1,0}$, Eq. (82) is valid in this case, too.

In the asymptotic approximation we have to substitute Eqs. (74)–(76) into Eq. (82). The products of trigonometric functions of phases $\psi_{1,2}$ can be presented as sums or differences of trigonometric functions of $\psi_1 + \psi_2$ and $\psi_1 - \psi_2$,

e.g., $\sin\psi_1 \cos\psi_2 = 1/2[\sin(\psi_1 + \psi_2) + \sin(\psi_1 - \psi_2)]$. We ignore terms varying with the rapidly changing phase $\psi_1 + \psi_2$ which nearly cancels out upon integration. We see that only modes with not too large difference of the radial orders n couple effectively because only then the phase difference changes slowly. The final formula for the coupling coefficient is obtained after keeping the dominant terms in $\Lambda_{1,2}$

$$\begin{aligned}
H = & \frac{Z\mathcal{D}_1\mathcal{D}_2}{4} \int \frac{dr}{r\sqrt{\kappa_1\kappa_2}} \left\{ \cos(\psi_2 - \psi_1) \left[y_{1,0} \left(\frac{\mathcal{A}}{\mathcal{C}} (4 + \mathcal{C}\sigma_0^2 - U - V_g) + \right. \right. \right. \\
& \qquad \qquad \qquad \left. \left. \left. + 2\sigma_1\sigma_2(2 - V_g) - \kappa_1\kappa_2\sigma_1\sigma_2 \frac{\Lambda_1 + \Lambda_2 - \Lambda_0}{\Lambda_1\Lambda_2} \right) + \right. \right. \\
& \qquad \qquad \qquad \left. \left. + y_{2,0} \left(\left(\frac{\mathcal{A}}{\mathcal{C}} + 2\sigma_1\sigma_2 \right) \left(V_g - \frac{\Lambda_0}{\mathcal{C}\sigma_0^2} \right) + \frac{\kappa_1\kappa_2\sigma_1\sigma_2}{2\mathcal{C}\sigma_0^2} \frac{(\Lambda_1 - \Lambda_2)^2 - \Lambda_0^2}{\Lambda_1\Lambda_2} \right) - \right. \right. \\
& \qquad \qquad \qquad \left. \left. - y_{3,0} V_g \left(\frac{\mathcal{A}}{\mathcal{C}} + 2\sigma_1\sigma_2 \right) - y_{4,0} \frac{\mathcal{A}}{\mathcal{C}} \right] + \right. \\
& \qquad \qquad \qquad \left. + \sin(\psi_2 - \psi_1) \left[y_{1,0} \left(\left(2\sigma_1\sigma_2 + \frac{\sigma_2^2}{\sigma_0^2} \frac{\mathcal{A}}{\mathcal{C}} \right) \frac{\kappa_2}{\Lambda_2} \frac{\Lambda_0 + \Lambda_2 - \Lambda_1}{2} - \right. \right. \right. \\
& \qquad \qquad \qquad \left. \left. \left. - \left(2\sigma_1\sigma_2 + \frac{\sigma_1^2}{\sigma_0^2} \frac{\mathcal{A}}{\mathcal{C}} \right) \frac{\kappa_1}{\Lambda_1} \frac{\Lambda_0 + \Lambda_1 - \Lambda_2}{2} \right) + \right. \right. \\
& \qquad \qquad \qquad \left. \left. + y_{2,0} \left(\left(\sigma_1^2 - \frac{1}{\mathcal{C}} + \frac{\sigma_2^2}{\sigma_0^2} \frac{1 - \mathcal{A}}{\mathcal{C}} \right) \frac{\kappa_2}{\Lambda_2} \frac{\Lambda_0 + \Lambda_2 - \Lambda_1}{2} - \right. \right. \right. \\
& \qquad \qquad \qquad \left. \left. \left. - \left(\sigma_2^2 - \frac{1}{\mathcal{C}} + \frac{\sigma_1^2}{\sigma_0^2} \frac{1 - \mathcal{A}}{\mathcal{C}} \right) \frac{\kappa_1}{\Lambda_1} \frac{\Lambda_0 + \Lambda_1 - \Lambda_2}{2} \right) \right] \right\}. \tag{83}
\end{aligned}$$

To obtain the expression for the coupling coefficient, C , we still need the asymptotic formula for the moments of inertia. Using Eqs. (73)–(76) in the general expression,

$$I_k = \int |\boldsymbol{\xi}_k|^2 \rho dV = \int |Y_k|^2 d\Omega \int (y_{1,k}^2 + \Lambda_k z_k^2) \rho r^4 dr,$$

we get

$$I_k = \frac{\mathcal{D}_k^2}{2} \int |Y_k|^2 d\Omega \int \left(\frac{1}{\kappa_k^2} + \frac{1}{\Lambda_k} \right) d\psi_k. \tag{84}$$

We adopt the normalization of spherical harmonics such that the angular integral in Eq. (84) is equal 4π . Together with the standard normalization of radial eigenfunctions, $y_{1,0}(R) = 1$, this gives us a simple interpretation of the amplitude A_0 (see Eq. 72). Its absolute value, B_0 , is then the surface averaged value of the $\delta R/R$ amplitude. Now, looking at Eqs. (3),(83),(84), we see that the coefficient C is independent of $\mathcal{D}_{1,2}$. It is also almost independent of gravity mode degrees, $l_{1,2}$, in the limit of $l_{1,2} \gg l_0$. The dependence on l_0 and m_0 remains. The latter comes only from the angular integral Z (see Dziembowski 1982 for explicit expressions).

Only some sets of values of angular degrees give the nonzero coupling. The case of $Z = 0$ takes place if $|l_2 - l_1| > l_0$ or if $(-1)^{l_2 - l_1} \neq (-1)^{l_0}$. Since we study

acoustic modes with $l_0 \leq 2$ we need to consider the cases $l_2 = l_1$ for $l_0 = 0$ modes, $l_2 = l_1 + 1$ for $l_0 = 1$ modes, and $l_2 = l_1$ and $l_2 = l_1 + 2$ for $l_0 = 2$ modes. Additionally, the azimuthal numbers m have to satisfy the condition $m_0 = m_1 + m_2$.

In our numerical calculations for each acoustic mode we consider a set of inner g-mode pairs of l_1 in the range from 40 to 1000, and for each l_1 the range of $\Delta n \equiv n_2 - n_1$ is from -20 to 20 . Furthermore, for each $(l_1, \Delta n)$ pair we consider various (m_1, m_2) pairs giving nonzero coupling coefficient. The dependence on l_1 is indeed weak and is illustrated in Fig. 8 for the lowest unstable radial mode and $l_0 = 2, m_0 = 0$ mode with $\sigma_0 = 3.883$.

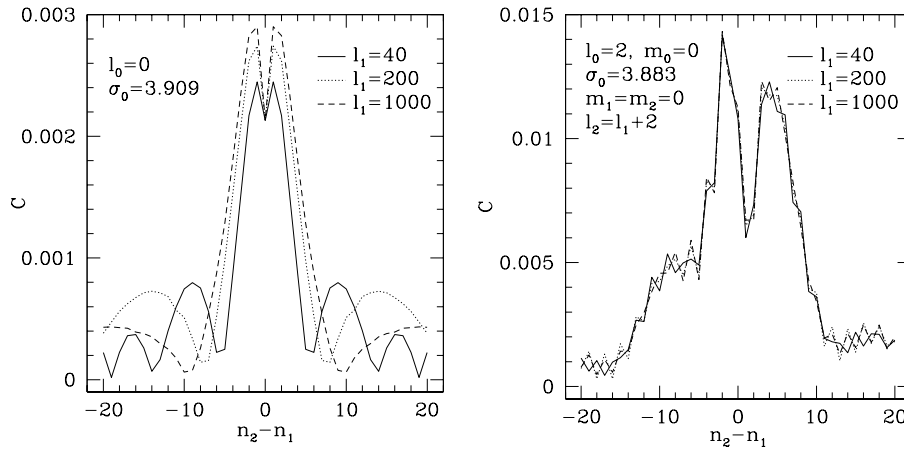


Fig. 8. The coupling coefficient C for the inner g-mode pairs and the lowest unstable radial mode (left panel) and $l_0 = 2, m_0 = 0, \sigma_0 = 3.883$ mode (right panel). In the latter case $l_2 = l_1 + 2$ and the g-mode azimuthal degrees are $m_1 = m_2 = 0$ which give maximum value of $|Z|$ for these l -values.

For the radial mode (left panel) most of the coupling comes from the region of a broad maximum of the Brunt-Väisälä frequency, $0.1 \lesssim r/R \lesssim 0.5$ and if the modes 1,2 have different frequencies, their propagation zones have different sizes. These differences decrease with increasing l_1 since the spectra densities increase. This is the cause of a bit different Δn -dependence of the coupling coefficients for different l_1 .

The two lowest $l_0 = 2$ modes (one of them is in the right panel) are in fact mixed modes with quite large values of eigenfunctions in the deepest part of the radiative region. Then, most of the coupling comes from the region $r/R < 0.1$, and the coupling coefficient is almost independent of the upper limit of the propagation zone. Therefore, the coupling coefficient dependence on Δn is nearly the same for different l_1 numbers.

We can also see in the plot that if $l_1 = l_2$ (left panel) the coupling coefficient is symmetric about $n_2 - n_1 = 0$. It is expected because the change of the sign of Δn means just interchange of the two g-modes and the coupling coefficient is symmetric with respect to it. Obviously, this is not true for $l_1 \neq l_2$ (right panel).

The coupling coefficients have maxima near $n_1 = n_2$ for each set of $l_0, \sigma_0, l_2 - l_1$.

For the radial modes these maxima are between 2.7×10^{-3} at $\sigma_0 = 3.909$ and 1.3×10^{-3} at $\sigma_0 = 5.859$. In the case of $l_0 = 1, m_0 = 0$ the maxima are between 1.1×10^{-3} at $\sigma_0 = 4.125$ and 0.4×10^{-3} at $\sigma_0 = 6.162$. For $l_0 = 1, |m_1| = 1$ the coupling coefficients are about 30% larger due to larger values of Z . For $l_0 = 1$, the values of coupling coefficients are a few times lower than in the case of radial modes due to lower p-mode amplitudes in the g-mode cavity. See also Fig. 9.

As has already been mentioned, in the case of $l_0 = 2$ we have to consider $l_2 = l_1$ together with $l_2 = l_1 + 2$. Typically, the $l_2 = l_1 + 2$ case is more important because the coupling coefficients are higher. The coupling coefficient maxima at $m_0 = 0$ and $m_0 = 1$ are between about 1.4×10^{-2} at $\sigma = 3.883$ and 1×10^{-3} at $\sigma_0 = 5.793$ while for $m_0 = 2$ the maxima are higher by a factor ~ 1.5 . The coupling coefficients for the two lowest $l_0 = 2$ modes are significantly larger than the coefficients for the remaining modes because these two modes have mixed character and high values of eigenfunctions in the region around $r/R = 0.1$.

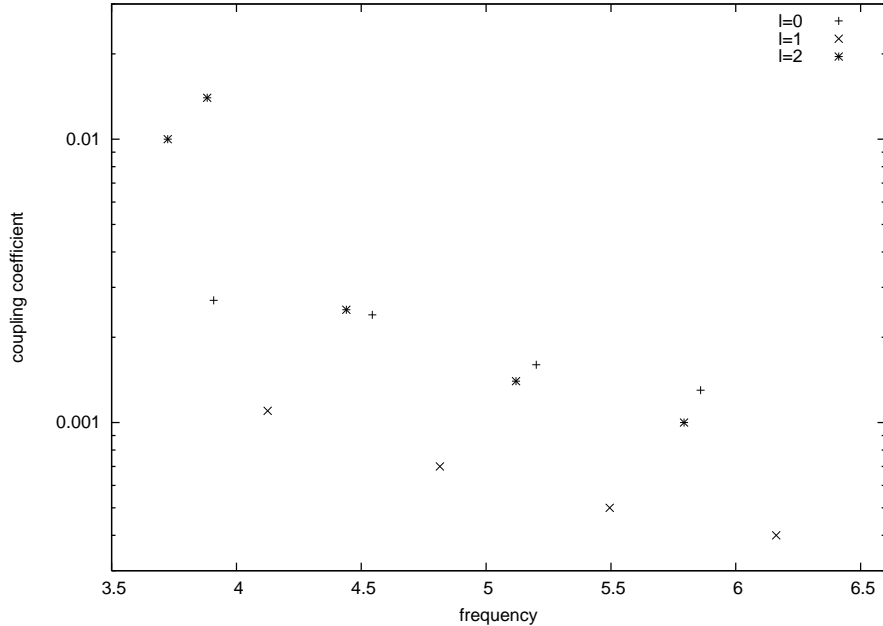


Fig. 9. The coupling coefficients maxima for the acoustic modes with $m = 0$. For $l = 1, m = 1$ the coupling coefficients are about 30% higher than those for $l = 1, m = 0$. For $l = 2, m = 1$ the coupling coefficients are similar to those at $l = 2, m = 0$. For $l = 2, m = 2$ the coupling coefficients are higher about the factor ~ 1.5 than those for $l = 2, m = 0, 1$.

In the case of the outer gravity modes we have to use Eq. (82) for H and the general expression for the moment of inertia. The angular degree dependence is the same as for the inner g-modes. It turns out that only modes with frequencies $\sigma_{1,2} \approx \sigma_0/2$ and $n_{1,2} = 1$ are important. The estimated values of coupling coefficients for the modes in Table 1 range from about 7 at $\sigma_0 \lesssim 4$ to about 40 at $\sigma_0 \gtrsim 5.5$. We should stress that these values should be treated as rough estimates, thus we do not give precise values.

5.4 Detuning Parameters and Critical Amplitudes

Apart of damping rates and coupling coefficients we need values of the detuning parameters, $\Delta\sigma$. We notice first that in the absence of rotation the mode frequencies are independent of m . This means that the detuning parameters are independent of m , too. It is important because each set l_0, m_0, l_1, l_2 characterizes whole multiplet of g-mode pairs. The pairs within the multiplet differ by m numbers of g-modes, but each pair has the same value of $m_1 + m_2$. The pairs in the multiplet have the same values of $\Delta\sigma$, so, in view of what was said previously about synchronization, we may treat whole multiplet as a single pair. If $l_0 \neq 0$ the pairs within the multiplet have different coupling coefficients, so we take into account only pair with the maximum value of the coefficient.

The inner g-modes with given angular degree, l , and different radial orders, n , form dense frequency spectra. In such a case the determination of the detuning parameter would require an unrealistically precise knowledge of the eigenfrequencies. Instead, we adopt statistical approach. For each g-modes' angular degree, l , we make a random choice of position of the frequency spectrum relative to the frequency of the acoustic mode. Then we compute detuning parameters for various g-mode pairs. The relatively strong coupling takes place only for $n_1 \approx n_2$ so we may neglect $|n_1 - n_2| \gtrsim 10$ (see Fig.8). This means also that the relevant pairs have $\sigma_1 \approx \sigma_2$. Moreover, we explain below that only one pair for each (l_1, l_2) is important.

At given l the frequencies of g-modes with consecutive n may be treated as equidistant in a relevant range of radial orders. Since $l_1 \approx l_2$ and $n_1 \approx n_2$, we have from Eq. (78) $\delta\sigma_{l_1, n_1} \approx \delta\sigma_{l_2, n_2}$, and

$$\begin{aligned} \Delta\sigma_{l_1, n_1+1, l_2, n_2-1} &= \sigma_0 - (\sigma_{l_1, n_1+1} + \sigma_{l_2, n_2-1}) \approx \\ &\approx \sigma_0 - (\sigma_{l_1, n_1} - \delta\sigma_{l_1, n_1} + \sigma_{l_2, n_2} + \delta\sigma_{l_2, n_2}) \approx \\ &\approx \Delta\sigma_{n_1, n_2}. \end{aligned} \quad (85)$$

This implies that all the relevant pairs with even $n_1 - n_2$ have close detuning parameters and may be treated as synchronized. As was explained in Section 4 such pairs may be treated as one effective pair with the coupling coefficient equal to the maximum value among even $n_1 - n_2$ pairs. Obviously, the same is true for odd $n_1 - n_2$ pairs. Finally, because

$$|\min(\Delta\sigma)_{\text{even } n_1 - n_2} - \min(\Delta\sigma)_{\text{odd } n_1 - n_2}| \approx \delta\sigma_{l_1, 2, n_1, 2}$$

is much higher than γ_0 for the relevant g-mode pairs, *i.e.*, those with l of the order of a few hundreds (Eq. 78), we may take into account only this pair which has smaller $|\Delta\sigma|$. The other one has too high detuning parameter and is not excited.

Even the lowest value of $|\Delta\sigma|$ is often much higher than γ_0 , and then we totally neglect g-mode pairs at a given (l_1, l_2) . What remains and is taken to further computations are single pairs at some values of l_1 .

It turns out that the most important pairs are in the range $100 \lesssim l_{1,2} \lesssim 300$. The lower- l pairs are negligible for two reasons. First, their spectrum is sparse

and few of them have $\Delta\sigma \sim \gamma_0$. Second, they have very small damping rates, which implies they hardly contribute to the overall damping (Eq. 48). On the other hand the pairs with high $l_{1,2}$ are strongly damped and turn out to be inactive in time-dependent solutions.

When the rotation is taken into account, the number of independent pairs increases due to splitting of g-mode frequencies. This effect will be studied in more details in Subsection 5.5.2.

In the case of the outer g-modes the damping rates are much higher than the acoustic mode driving rates. This implies that only one pair suffices to halt the acoustic mode growth and the system reaches the limit cycle solution, similar to that studied in Subsection 3.1. In this case the critical amplitude (Eq. 7) is a good estimate of the average acoustic mode amplitude. This critical amplitude is insensitive to the detuning parameter because it is much smaller than the damping rate and may be neglected in Eq. (7). This also implies that taking into account rotation does not change the expected acoustic mode amplitude.

The outer g-mode pairs have to be taken into account if the average acoustic mode amplitude determined by the interaction with only the inner g-mode pairs is higher than the critical amplitude for the excitation of the outer g-mode pair. In particular, such a situation takes place for the acoustic modes with relatively high growth rates, because then many inner g-mode pairs are necessary to halt the driving. The detuning parameters of those pairs are also relatively high. Even though there is no simple dependence of resulting average acoustic mode amplitude on detuning parameters of active inner g-mode pairs, the qualitative dependence is similar as in the single-pair case, *i.e.*, the higher detuning parameters are, the higher the amplitude is. In our model, higher frequency acoustic modes have high growth rates and we expect high average amplitudes determined by the interaction with the inner g-modes. Then, the outer g-mode pairs may dominate the interaction.

5.5 Time Evolution

5.5.1 The Case of Slow Rotation

In the case of sufficiently slow rotation, the splitting of the g-modes is smaller than their damping rates and the multiplets may be treated as single modes, as was explained in Subsection 3.3. Here we study a few examples of such systems. In all cases we set $m_0=0$. Other values of m_0 give slightly different values of coupling coefficients, which results only in slight change of the amplitudes. Indeed, if we increase the coupling coefficients in Eqs. (30)–(32) by some factor and decrease the amplitudes by the same factor, the equations will remain unchanged. This means the amplitude values scale with coupling coefficients without change of the time dependence which is governed by the p-mode growth rate.

At first, we consider the $l_0=2, \sigma_0=3.883$ mode together with an ensemble of several hundred inner g-mode pairs in the l_1 -range between 40 and 1000. The beginning of the time evolution of the acoustic mode amplitude is shown in Fig. 10. The initial value of the amplitude is set to be equal to the low-

est critical amplitude. The initial g-mode energies were randomly distributed between zero and the acoustic mode initial energy. At the very beginning the acoustic mode amplitude drops as the result of the interaction with hundreds of artificially excited g-modes. Then, the modes become temporarily uncoupled and g-mode amplitudes fall down, while the acoustic mode amplitude starts to grow exponentially. Next, several g-mode pairs become excited due to the interaction with the acoustic mode and a statistical equilibrium is reached after about 5×10^4 days. The average amplitude in this state is about 0.001 and average modulation period is about 3000 days. It is of the order of $1/\gamma_0 \approx 5600$ days. Only inner g-modes actively interact with the acoustic mode.

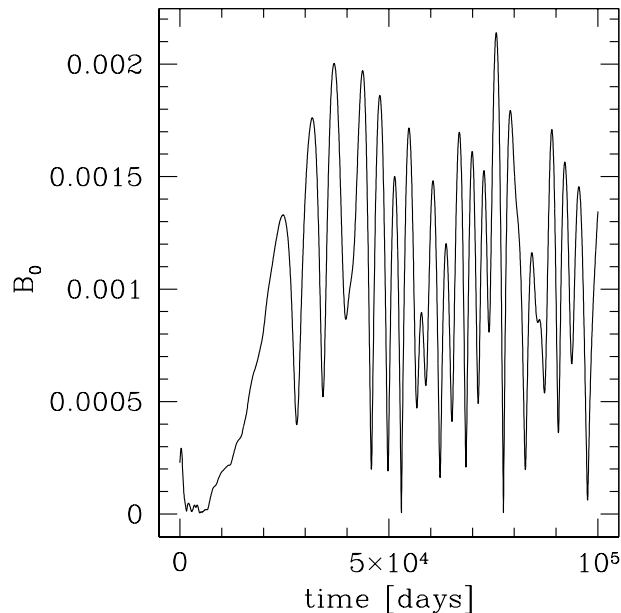


Fig. 10. The time evolution of the $l_0=2, \sigma_0=3.883$ acoustic mode amplitude.

The $l_0=2, \sigma_0 < 4$ modes are not typical unstable modes in our model. They are, in fact, mixed modes with significant amount of energy concentrated in the internal g-mode cavity. This causes strong coupling to the inner g-modes and weak linear driving, the latter being the result of a large mode inertia. Therefore, we performed the same time integration for the radial $\sigma_0 = 3.909$ mode. Although the outer g-modes should be taken into account in this case, we first consider only inner g-modes in order to compare the results with the previous case when the growth rate was significantly smaller.

The time evolution of the radial mode amplitude in the statistical equilibrium without outer g-modes is presented in Fig. 11. We see that the average amplitude is about 0.01 and the typical modulation period is about 1000 days. This timescale is again of the order of $1/\gamma_0 \approx 1600$ days. The amplitude is about 10 times higher than in the case in Fig. 10, mainly due to coupling coefficients

which are smaller by a factor of 5. The remaining factor of 2 turns out to be the result of dependence of the average amplitude on the growth rate. This dependence is expected because γ_0 determines $\Delta\sigma$ range of active g-mode pairs and, as in the case of a single pair, there is some dependence of the average amplitude on detuning parameters.

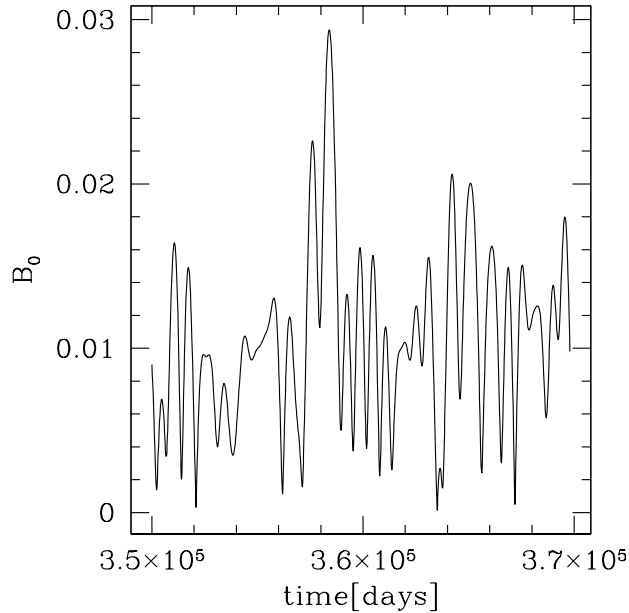


Fig. 11. The time evolution of the $l_0=0, \sigma_0=3.909$ acoustic mode amplitude without outer g-modes.

The time evolution of the same radial mode with the outer g-modes taken into account is presented in Fig. 12. There is a qualitative difference in amplitude behavior between this case and the previous one. This difference is caused by the presence of outer g-modes which are strongly damped and strongly coupled to the radial mode. The sudden jumps of amplitude, lasting less than 10 days, coincide with very short time intervals during which the outer g-mode is excited.

Different behavior of the modes in this case than in the previous ones is caused by orders-of-magnitude larger ratio $|\gamma_{1,2}|/\gamma_0$ of the dominant g-modes. Some of the inner g-mode pairs also remain excited, which is manifested by smooth amplitude changes, *e.g.*, around 3.12×10^5 days. However, the inner g-modes play a secondary role in this case. In spite of different behavior of the amplitude, the modulation timescale is similar to that in the case without inner g-modes. This is the manifestation of the fact that also in this case the timescale is governed by the acoustic mode growth rate.

This case resembles the case of a single g-mode pair, because only one pair is sufficient to stabilize the acoustic mode. The average amplitude of the latter

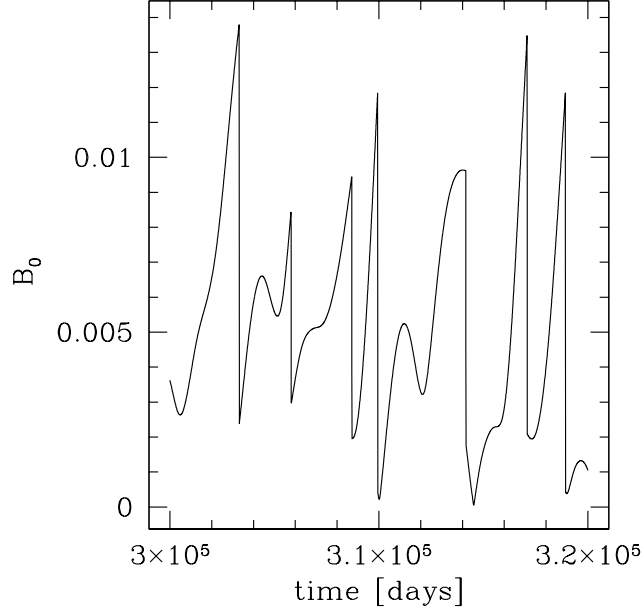


Fig. 12. The time evolution of the $l_0 = 0, \sigma_0 = 3.909$ acoustic mode amplitude with outer g-modes.

is of the order of the critical amplitude to the excitation of the outer g-mode, equal approximately 0.005. This value is smaller than the average amplitude in the previous example, *i.e.*, determined by inner g-modes and equal ~ 0.01 . Therefore, the interaction with the outer g-mode dominates.

The last example is the case of the $l_0 = 1, \sigma_0 = 5.495$ acoustic mode which is one of the most strongly unstable modes and for which the coupling to the inner g-modes is one of the weakest. The time evolution of this mode is shown in Fig. 13. Only an outer g-mode pair remain effectively interacting after several hundred days. The system converges to the periodic limit cycle with this pair. Very short modulation timescale, about 100 days, is caused by very high growth rate, $1/\gamma_0 \approx 50$ days.

The high value of γ_0 demands many weakly damped inner g-mode pairs to stabilize the system. Moreover, these modes are very weakly coupled to the acoustic mode and, consequently, the resulting average amplitude of the latter would be much higher than ~ 0.02 , *i.e.*, the critical amplitude for the excitation of the outer g-mode pair. Therefore, the outer g-mode pair strongly dominates the interaction and we cannot even notice the presence of the inner g-mode pairs.

Other unstable acoustic modes have average amplitudes similar to those in the last two cases, *i.e.*, of the order of $0.01 \div 0.02$, and the interaction is dominated by the outer g-modes.

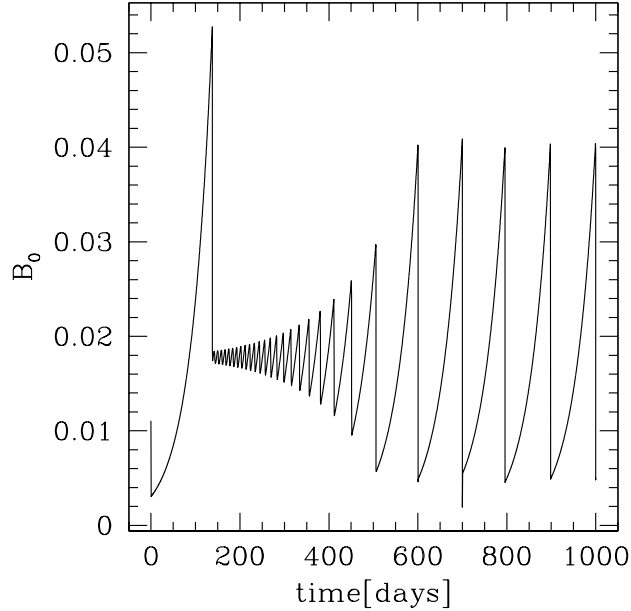


Fig. 13. The time evolution of the $l_0 = 1, \sigma_0 = 5.495$ acoustic mode amplitude.

5.5.2 The Case of Moderate and Fast Rotation

Since the modes of close frequencies effectively act as independent only if the $\Delta\sigma$ -separation is sufficiently large, rotational splitting may significantly change the picture only if rotation is fast enough. In this section we will try to determine the critical rotation rate at which modes can be treated as independent. In Subsection 3.3 we showed that the separation must exceed γ for pairs to be regarded independent.

Now, let us consider $\Delta\sigma$ separation between members of g-mode multiplets that may be coupled to low-degree acoustic mode. Very good approximation for the high- l inner g-mode's eigenfrequency in the corotating frame, up to quadratic terms in rotation is (Dziembowski *et al.* 1988)

$$\sigma_{\text{rot}} \approx \sigma_{\text{nrot}} + \frac{m\Omega_{\text{rot}}}{l^2} - \frac{m^2\Omega_{\text{rot}}^2}{l^2\sigma_{\text{nrot}}}, \quad (86)$$

where Ω_{rot} is dimensionless rotational frequency of a star. The g-modes in each pair have angular degrees $l_1 \approx l_2$ and $m_1 \approx -m_2$ so we neglect the difference in linear terms in rotation in the formula for the detuning parameter

$$\Delta\sigma_{\text{rot}} \approx \Delta\sigma_{\text{nrot}} + \frac{4}{\sigma_0} \left(\frac{m_1\Omega_{\text{rot}}}{l_1} \right)^2, \quad (87)$$

where we used $\sigma_{\text{nrot}} \approx \sigma_0/2$. The rotational frequency change of the acoustic mode is unimportant here, since it only shifts all the detuning parameters by the

same value, without changing their statistical properties. The rotation begins to be important when

$$\Omega_{\text{rot}}^2 > \frac{|\gamma_{l_1}| \sigma_0}{4}. \quad (88)$$

In the numerical experiments from the previous subsection with only inner g-modes taken into account, the typical l of active pairs was 200. Thus, from Eq. (88) we find that the rotation becomes important at $\Omega_{\text{rot}} \gtrsim 0.001$. Assuming uniform rotation of the star, this value in our model corresponds to equatorial velocity below 1 km/s.

The linear terms in rotation are higher than the quadratic ones for very small rotation rate and $l_1 \neq l_2$. However, at $l_0 = 2$ and $l_1 \sim 10^2$ we estimated that the linear $\Delta\sigma$ -splitting exceeds the quadratic one at rotation rate smaller than 0.4×10^{-3} . At such low values the splitting is smaller than $|\gamma_l|$ so the rotation is negligible. When the rotation becomes significant, only quadratic terms play role.

In order to assess terminal amplitude of acoustic mode in the presence of rotation we performed a number of numerical experiments. To reduce the number of g-mode pairs we divide each multiplet into groups of pairs such that detuning parameters in each group differ less than the value of the damping rate,

$$|\Delta\sigma_{l,m} - \Delta\sigma_{l,m'}| < |\gamma_l|. \quad (89)$$

Each group of pairs is treated as a single pair with mean detuning parameter and coupling coefficient equal the maximum one within the group. We ignored the influence of rotation on the coupling coefficients. The detuning parameters of different groups differed more than the damping rate of the multiplet. In particular, in the absence of rotation whole multiplet formed one group of pairs and was thus replaced by a single pair.

An example of the time evolution of the $l_0 = 0, \sigma_0 = 3.909$ mode amplitude with the rotation frequency $\Omega_{\text{rot}} = .01$ is presented in Fig. 14. We see that the average amplitude is about 0.0025. It is about factor of ~ 4 lower than in the case without rotation (see Fig. 11). Moreover, the characteristic timescale is somewhat longer than in the case without rotation. This is the result of much denser $\Delta\sigma$ spectrum of active pairs. The dense spectrum implies that there are many independent low- l pairs in the vicinity of exact resonance and there is no need to excite pairs with higher $\Delta\sigma$. Consequently, the modulation timescales are shorter, but still they are of the order of $1/\gamma_0$.

The transition from no rotation to fast rotation is shown in Fig. 15. At very slow rotation its influence on the average amplitude is negligible. The rotation becomes significant at $\Omega_{\text{rot}} \approx 0.002$ which is of the order of the simple estimate obtained above. Further increase of the rotation rate causes that the average acoustic mode amplitude decreases. Above $\Omega_{\text{rot}} \approx 0.01$ the effect of rotation saturates. We may treat the rotation rate at which the average amplitude is reduced by the factor of 2 as the limit between slow and fast rotation. This limit in our case is $\Omega_{\text{rot}} \approx 0.003$. Assuming uniform rotation this value corresponds to equatorial velocity about 2 km/s.

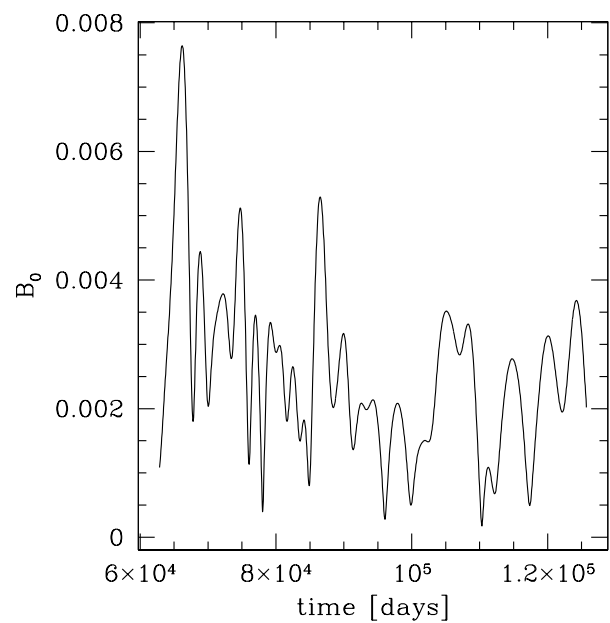


Fig. 14. The time evolution of the $\sigma_0 = 3.909$ radial mode interacting with the g-mode pairs in the presence of rotation, $\Omega_{\text{rot}} = 0.01$.

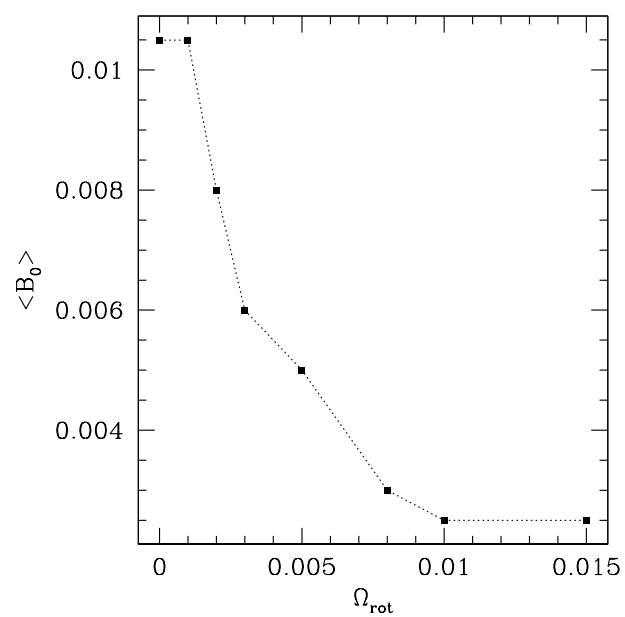


Fig. 15. Average amplitude of the $\sigma_0 = 3.909$ radial mode interacting with the inner g-modes versus dimensionless stellar rotation rate.

If we take into account outer g-modes it turns out that they dominate at slow rotation (see previous subsection). At fast rotation inner g-modes are able to limit amplitude growth of the radial mode at values below critical ones for outer g-modes which thus remain unexcited.

The role of rotation is important for the p-modes whose amplitudes are determined by the interactions with the inner g-modes. In our model they are weakly unstable $l_0=2, \sigma_0 < 4$ modes. Their amplitudes are reduced by the factor of a few due to fast rotation.

On the other hand, for high frequency p-modes ($\sigma_0 > 4$) even fast rotation cannot change the situation, because even at the fastest rate the outer g-modes must be excited and they determine the p-mode amplitudes. As was explained in Subsection 5.4, the outer g-modes are insensitive to rotation. Thus the values of the amplitudes of the $\sigma_0 > 4$ p-modes are the same as in Subsection 5.5.1, *i.e.*, of the order of $0.01 \div 0.02$.

5.6 Luminosity Amplitudes

In order to obtain the expected luminosity amplitudes, we have to multiply radius variations amplitudes by a nonadiabatic coefficient f . As was mentioned in Subsection 5.1, the absolute value of this coefficient for all considered acoustic modes is about 30. The effects of flux averaging over the stellar disc play role mainly for $l=2$ modes, and they reduce effective $|f|$ to the value of about 20. Moreover, for the modes whose radius amplitudes are determined by the interaction with the inner g-modes, we adopt the values obtained at fast rotation.

In the case of radial acoustic modes the evaluated bolometric luminosity amplitudes range from about 0.07 mag at $\sigma = 3.909$ to more than 0.5 mag at $\sigma = 5.859$. Only the $\sigma = 3.909$ radial mode has amplitude determined by the interaction with the inner g-modes and the value of the amplitude is calculated with the rotation taken into account.

All the $l=1$ acoustic modes have amplitudes determined by the outer g-modes. The values of the amplitudes range from ~ 0.15 mag at $\sigma = 4.125$ to more than 0.5 mag at $\sigma > 5$.

The $l=2$, acoustic modes with $\sigma < 4$ have relatively small expected luminosity amplitudes, about 5 mmag. This is the combined result of their low growth rates, strong coupling to the inner g-modes, fast rotation and disc-averaging effect. However, at $\sigma > 4$ the expected amplitudes are again high, of the order of a few tenths of a magnitude.

Comparing obtained luminosity amplitudes with those observed in XX Pyx or other δ -Scuti stars, we see that only low-frequency $l=2$ modes in our model have expected amplitudes below 10 mmag. Higher frequency acoustic modes have amplitudes equal a large fraction of a magnitude. These values are typical for HADS stars. Neglecting outer g-modes results in even higher amplitudes. This suggests that nonresonant saturation effects play an important role in limiting the amplitudes. However, at present stage we cannot exclude the possibility that our treatment of the outer g-modes is too crude and more realistic modeling of those modes would give better consistency with observations.

5.7 Effects of Saturation of The Linear Driving

The saturation of the instability mechanism is manifested by the nonlinear dependence of the growth rates on mode amplitudes. The nonlinear growth rates may be written in the form (see, *e.g.*, Buchler and Goupil 1984)

$$\gamma_k^{\text{nl}} = \gamma_k^{\text{lin}} \left(1 + \sum_j S_{k,j} B_j^2 \right), \quad (90)$$

where $S_{k,j} < 0$ are saturation coefficients and the summation is made over all modes excited in the star.

The simplest way to consider the saturation mechanism is to reduce the values of the growth rates. Then, as implied by Eq. (48), the number of g-modes necessary to achieve the statistical equilibrium is reduced, too. The lower driving rate, as we explained in Section 4, means also that the $\Delta\sigma$ range of active pairs is smaller. Consequently, the expected amplitude of the acoustic mode becomes lower and the modulation timescale is longer.

The effect of the growth rate saturation is relevant only in the interaction with the inner g-modes. For the outer g-modes there is no reduction of the amplitude because the damping rate is always much higher than the growth rate.

The cases of very small growth rates were studied by Dziembowski and Królikowska (1985) and Dziembowski *et al.* (1988). The amplitude of the acoustic mode is then given by the lowest critical amplitude (Eq. 7) for the whole ensemble of the resonant g-mode pairs. It is so, because the pair corresponding to this minimum is able to halt the acoustic mode growth. The system reaches the stable equilibrium, described in Section 2.1.2, or a periodic limit cycle such as described in Section 3.1. The expected amplitude of the acoustic mode in both situations is close to the critical one.

For the XX Pyx the simple assessment based on Eq. 7 with the rotation and strong saturation taken into account and the respective f coefficient leads to amplitude ranging from about 1 mmag at $l=2, \sigma < 4$ modes up to about 0.1 mag at $l=1, \sigma > 5$ modes. The amplitudes of the high frequency acoustic modes are still much larger than observed in XX Pyx. The fact that we find amplitudes considerably higher than Dziembowski and Królikowska (1985) did, is a consequence of evolved δ Scuti star model while they used a ZAMS star model. In our case the inner g-modes are more concentrated at the peak of the Brunt-Väisälä frequency below $r=0.1R$ and consequently they are much more weakly coupled to the p-mode. The interaction with the outer g-modes is also weaker in our case because of higher damping rates.

The unavoidable conclusion is that the dominant effect responsible for the amplitude limitation in δ Scuti stars must be nonlinear saturation. In such a situation our basic approximation that acoustic modes remain uncoupled is not allowed. The coupling between various acoustic modes occurs through the collective saturation of the driving mechanism, as described by Eq. (90). The decrease of amplitudes of certain modes gives the chance for other modes to be

excited. The net effect depends on the linear growth rates and the saturation coefficients. In Fig. 6. we see that the linear growth rates initially grow rapidly with frequency. However, the saturation coefficients are also growing with frequencies as both observations and hydrodynamical simulations show. The high frequency modes are both easy to excite and easy to saturate. It requires numerical calculations to predict the outcome of the collective saturation. The only thing that can be said at this stage is that the amplitude changes should be faster for high frequency modes.

6 Conclusions

We studied the resonant coupling between unstable acoustic modes and pairs of stable g-modes. We reminded the general analysis of the interaction given by Dziembowski (1982) and Dziembowski and Królikowska (1985). The most important properties of the interaction are such that a g-mode pair gets excited if the acoustic mode amplitude exceeds certain critical value, and that a three-mode equilibrium solution is stable if the acoustic mode driving is weaker than g-mode damping and if the detuning parameter is not too small. We also showed that the nonadiabacity of the nonlinear coupling does not change the problem qualitatively.

In the case of many g-mode pairs the equilibrium solution involving more than two pairs in general does not exist. Instead, we have a kind of statistical equilibrium involving many pairs exchanging energy with the acoustic mode. We showed that such a state may be stable if the sum of damping rates of active g-mode pairs is higher than the acoustic mode growth rate. Moreover, these g-mode pairs should be separated in the space of detuning parameters by more than their damping rates. The pairs that have close detuning parameters get synchronized and interact effectively as a single pair.

The separation of detuning parameters and the condition of the stability imply that the range of the detuning parameters of active pairs is of the order of the p-mode growth rate. The inverse of the growth rate determines the timescale of the modulation of the acoustic mode amplitude. The fast amplitude variations cause that the expression for the critical amplitude derived in quasi-static approximation is no longer applicable and many pairs are excited despite being stable according to the parametric instability criterion applied to the time-averaged p-mode amplitude.

We applied our theory to a seismic model of a δ Scuti star XX Pyx. We consider all unstable acoustic modes of $l \leq 2$. Their dimensionless frequencies, $\nu\sqrt{\pi/(G < \rho >)}$, are between, 3.7 and 6.2, corresponding to radial orders $n > 3$. Such modes couple to g-mode pairs that propagate either in the outer layers, $0.95 \lesssim r/R \lesssim 0.98$, or in the interior, $0.1 \lesssim r/R \lesssim 0.5$. The two groups of g-modes have very different properties, in particular the frequency spectra. While the number of the inner g-modes that can be excited due to the parametric instability is large, typically only one outer g-mode pair has to be taken into account. The outer g-modes are orders of magnitude more strongly damped

but also much more strongly coupled to the acoustic modes, resulting in critical amplitudes comparable to those for the inner g-modes.

The $l=2$ acoustic modes of low frequencies, $\sigma < 4$, reach statistical equilibria determined by the interactions with the inner g-modes of $l \sim 10^2$. The average amplitudes are below the critical values for the excitation of the outer g-modes which thus remain unexcited. The rotation causes that the average amplitudes are by the factor of a few lower than in the case without rotation. It is so because the rotation causes splitting of detuning parameters and above certain rate the pairs within multiplets loose synchronization and act independently. This increases the number of effectively interacting g-mode pairs and leads to lower acoustic mode amplitudes. The effect of rotation becomes significant already at equatorial velocity of the order of 1 km/s. Then, the average bolometric luminosity amplitudes are of the order of a few millimagnitudes. The typical modulation timescales are of the order of $10^3 \div 10^4$ days.

The $l=0$, $\sigma = 3.909$ mode has average amplitude determined mainly by the interaction with the outer g-mode pair, but the time behavior is affected by the presence of a few excited inner g-mode pairs. Effect of rotation is to increase the number of inner g-modes and these modes take control of the acoustic mode evolution. The average amplitude is now lower leading the outer g-modes unexcited. The rotation again turns out to be important already at rates ~ 1 km/s. Then the average bolometric luminosity amplitude is about 0.07 mag and the modulation timescale is of the same order as in the previous case, *i.e.*, 10^3 days

The amplitudes of high frequency acoustic modes, $\sigma > 4$, are determined solely by the interaction with the outer g-mode pairs. Typically, the system reaches periodic limit cycle solutions. The rotation has no effect in this case. The predicted bolometric luminosity amplitudes are large, much higher than observed. The modulation timescales are of the order of $10^2 \div 10^3$ days.

We found that the resonant mode coupling alone cannot be the main effect responsible for amplitude limitation in δ Scuti stars, at least in hotter and evolved ones as XX Pyx. Our calculated luminosity amplitudes are too high, in particular for high frequency modes. There is an obvious conflict with the observations.

A nonlinear saturation of the linear driving effect leads to a reduction of the acoustic mode amplitudes. If strong enough it may lead to constant amplitude pulsation such as discussed by Dziembowski and Królikowska (1985). However, in our application to an evolved δ Scuti star model the calculated amplitudes are still higher than observed. The difference between the two results is a consequence of the difference in the internal structure of the adopted models. We stressed that in the case when the dominant amplitude limitation mechanism is the nonlinear saturation, the coupling between unstable acoustic modes must be taken into account.

Acknowledgements. The author is very grateful to Prof. W. Dziembowski for creative and stimulating discussions as well as for useful comments concerning the text of this paper. This work was supported by the KBN grant No. 5

P03D 030 20.

REFERENCES

- Breger, M. 1979, *P.A.S.P.*, **91**, 5.
 Breger, M. 2000a, in: "Delta Scuti and Related Stars", *ASP Conf. Ser.*, 210, Eds. M. Breger and M. Montgomery, p. 3.
 Breger, M. 2000b, *MNRAS*, **313**, 129.
 Breger, M. *et al.* 1998, *Astron. Astrophys.*, **331**, 271.
 Buchler, J.R., Goupil, M.J. 1984, *Astrophys. J.*, **279**, 394.
 Davidson, R.C. 1972, *Methods in Nonlinear Plasma Theory*, New York: Academic Press.
 Dziembowski, W.A. 1977, *Acta Astron.*, **27**, 203.
 Dziembowski, W.A. 1982, *Acta Astron.*, **32**, 147.
 Dziembowski, W.A., Królikowska, M. 1985, *Acta Astron.*, **35**, 5.
 Dziembowski, W.A., Królikowska, M., Kosovitchev, A. 1988, *Acta Astron.*, **38**, 61.
 Handler, G., *et al.* 2000, *MNRAS*, **318**, 511.
 Kumar, P., Goodman, J. 1996, *Astrophys. J.*, **466**, 946.
 Moskalik, P. 1985, *Acta Astron.*, **35**, 229.
 Pamyatnykh, A.A., Dziembowski, W.A., Handler, G., Pikall, H. 1998, *Astron. Astrophys.*, **333**, 141.
 Rodriguez, E. 1999, *P.A.S.P.*, **111**, 709.
 Van Hoolst, T. 1993, *Astron. Astrophys.*, **279**, 417.
 Van Hoolst, T. 1994a, *Astron. Astrophys.*, **286**, 879.
 Van Hoolst, T. 1994b, *Astron. Astrophys.*, **292**, 471.
 Van Hoolst, T., Dziembowski, W.A., Kawaler, S.D. 1998, *MNRAS*, **297**, 536.
 Vandakurov, Y.V. 1965, *Proc. Acad. Sci. USSR*, **164**, 525.
 Vandakurov, Y.V. 1979, *Astron. Zhur.*, **56**, 749.
 Viskum, M. *et al.* 1998, *Astron. Astrophys.*, **335**, 594.
 Wersinger, J.M., Finn, J.M., Ott, E. 1980, *Phys. of Fluids*, **23**, 1142.